AD-A040 621 ARMY MISSILE RESEARCH DEVELOPMENT AND ENGINEERING LAB--ETC F/G 20/6
THE EFFECTS OF SPECKLE ON RESOLUTION OF HIGH CONTRAST AND CONTI--ETC(U)
DEC 76 C R CHRISTENSEN, A KOZMA

UNCLASSIFIED RR-77-2 NL

1 OF 1
ADA
040621

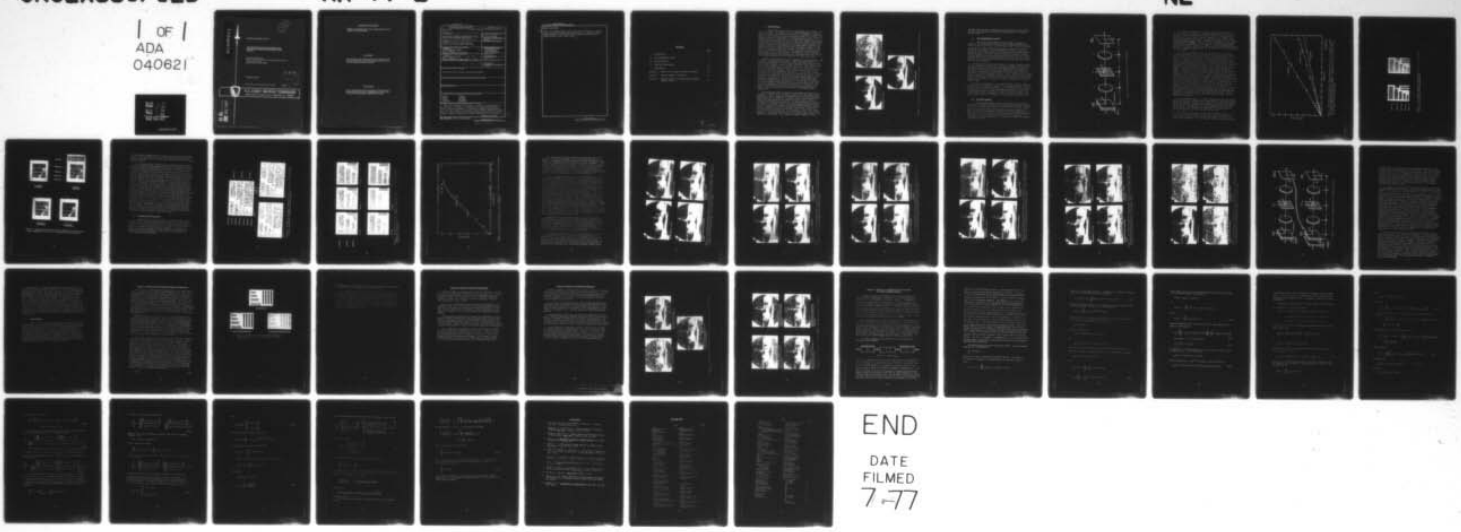

END

DATE
FILMED
7-77

TECHNICAL REPORT RR-77-2

THE EFFECTS OF SPECKLE ON RESOLUTION OF HIGH CONTRAST AND CONTINUOUS TONE OBJECTS

Physical Sciences Directorate
US Army Missile Research, Development and Engineering Laboratory
US Army Missile Command
Redstone Arsenal, Alabama 35809

14 December 1976

Approved for public release; distribution unlimited.

U.S. ARMY MISSILE COMMAND
Redstone Arsenal, Alabama 35809

DISPOSITION INSTRUCTIONS

DESTROY THIS REPORT WHEN IT IS NO LONGER NEEDED. DO NOT RETURN IT TO THE ORIGINATOR.

DISCLAIMER

THE FINDINGS IN THIS REPORT ARE NOT TO BE CONSTRUED AS AN OFFICIAL DEPARTMENT OF THE ARMY POSITION UNLESS SO DESIGNATED BY OTHER AUTHORIZED DOCUMENTS.

TRADE NAMES

USE OF TRADE NAMES OR MANUFACTURERS IN THIS REPORT DOES NOT CONSTITUTE AN OFFICIAL INDORSEMENT OR APPROVAL OF THE USE OF SUCH COMMERCIAL HARDWARE OR SOFTWARE.

UNCLASSIFIED

SECURITY CLASSIFICATION OF THIS PAGE (When Data Entered)

REPORT DOCUMENTATION PAGE

READ INSTRUCTIONS BEFORE COMPLETING FORM

1. REPORT NUMBER: RR-77-2	2. GOVT ACCESSION NO.
3. RECIPIENT'S CATALOG NUMBER	
4. TITLE (and Subtitle): THE EFFECTS OF SPECKLE ON RESOLUTION OF HIGH CONTRAST AND CONTINUOUS TONE OBJECTS	5. TYPE OF REPORT & PERIOD COVERED: Technical Report
6. PERFORMING ORG. REPORT NUMBER: RR-77-2	
7. AUTHOR(s): Charles R. Christensen and Adam Kozma	8. CONTRACT OR GRANT NUMBER(s)
9. PERFORMING ORGANIZATION NAME AND ADDRESS: Commander, US Army Missile Command, Attn: DRSMI-RR, Redstone Arsenal, Alabama 35809	10. PROGRAM ELEMENT, PROJECT, TASK AREA & WORK UNIT NUMBERS: DA 1W362303A214, AMCMS 632303.2141411
11. CONTROLLING OFFICE NAME AND ADDRESS: Commander, US Army Missile Command, Attn: DRSMI-RPR, Redstone Arsenal, Alabama 35809	12. REPORT DATE: 14 December 1976; 13. NUMBER OF PAGES: 45
14. MONITORING AGENCY NAME & ADDRESS (if different from Controlling Office)	15. SECURITY CLASS. (of this report): UNCLASSIFIED
	15a. DECLASSIFICATION/DOWNGRADING SCHEDULE

16. DISTRIBUTION STATEMENT (of this Report)

Approved for public release; distribution unlimited.

17. DISTRIBUTION STATEMENT (of the abstract entered in Block 20, if different from Report)

18. SUPPLEMENTARY NOTES

19. KEY WORDS (Continue on reverse side if necessary and identify by block number)

Imaging	Scanned
Speckle	Smoothing
Coherent	Averaging
Incoherent	Frequency

20. ABSTRACT (Continue on reverse side if necessary and identify by block number)

The effect of speckle in the imaging of diffusely illuminated gratings and continuous tone objects was studied. It was found that when imaging diffuse gratings the aperture of a coherently illuminated system must be 2.6 times as large as that of an incoherent system to obtain comparable resolution. This factor must be increased to five when imaging objects with a continuous spatial frequency distribution and range of contrast and to a factor of →

next page

ABSTRACT (Continued)

DD FORM 1 JAN 73 1473 EDITION OF 1 NOV 65 IS OBSOLETE

UNCLASSIFIED

SECURITY CLASSIFICATION OF THIS PAGE (When Data Entered)

400 625

ABSTRACT (Concluded)

cont →

seven if the coherent image is subsequently low-pass filtered. A coherent system can achieve resolution which is comparable to an incoherent system of equal aperture if the coherent image is smoothed so that the mean to standard deviation ratio is ten or more.

CONTENTS

		Page
I.	INTRODUCTION.	3
II.	THE EXPERIMENTAL SYSTEM	5
III.	GRATING IMAGING	5
IV.	CONTINUOUS TONE IMAGING	10
V.	CONCLUSIONS	23
Appendix A.	SPECKLE WITH COHERENT SCANNED ILLUMINATION	25
Appendix B.	SPECKLE AVERAGING TECHNIQUES	29
Appendix C.	SIGNAL-TO-NOISE RATIO FOR LOW-PASS FILTERED COHERENT IMAGES.	32

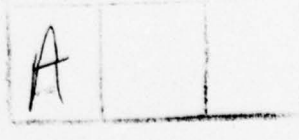

I. INTRODUCTION

When diffuse objects which are illuminated with coherent radiation are viewed, the appearance of the image is degraded by the presence of speckle. The effect of speckle is to superimpose a noise-like structure which masks the spatial information present in the image. The effect of speckle on image quality is demonstrated in Figure 1. The transparency shown at the bottom of the figure was imaged using the minimum optical system resolution (aperture) that would allow identification of the vehicle in the foreground when incoherent illumination was used. Images recorded when the transparency was illuminated by diffuse incoherent light and by diffuse coherent light are shown in Figure 1. The speckle in the image formed with coherent illumination makes it difficult to determine that the object in the foreground is an automobile; other objects in the image are also unrecognizable. With incoherent illumination, the type of automobile can be determined and other details such as the powerline and the structure of the tower can be seen.

Speckle occurs regardless of the wavelength of the illumination used as long as the radiation is coherent. Thus, the phenomenon can be observed in holography or in other imaging systems using lasers working in the visible region, in the microwave region with such systems as synthetic aperture radars, in the infrared region when using lasers, or even with ultrasonic imaging systems using coherent sound illumination. It is also important in imaging using a small coherent beam scanned over the object for illumination (Appendix A). In all these systems, the effect of the speckle is apparently to increase the size of the minimum resolution patch which can be obtained with a given aperture size compared to that which is obtained from the same size aperture using incoherent illumination. Because a number of important advantages accrue from using coherent illumination, it is important to understand how speckle affects resolution and, in turn, the recognition and identification capability of coherent imaging systems. A number of techniques can be used for smoothing the speckle in coherent imagery in order to improve resolution to approach that of incoherent imagery (Appendix B).

The deleterious effect of speckle on resolution has been noted by a number of workers [1-6]. Recently, Young, et al. [6] performed some experiments, using a diffusely illuminated National Bureau of Standards (NBS) target and an optometrists tumbling E chart, which showed that speckle degrades resolution by a factor of five or more. The work presented here extends those results. The aperture required to resolve a coherently illuminated diffuse grating is determined and compared to the aperture required to resolve the grating using incoherent illumination. In addition, an estimate is made of the degree of incoherent averaging needed to improve the resolving power of the coherent image to a point which approaches that of an incoherent system. The aperture required to resolve diffuse continuous tone objects using coherent illumination is determined. These results are again compared to those

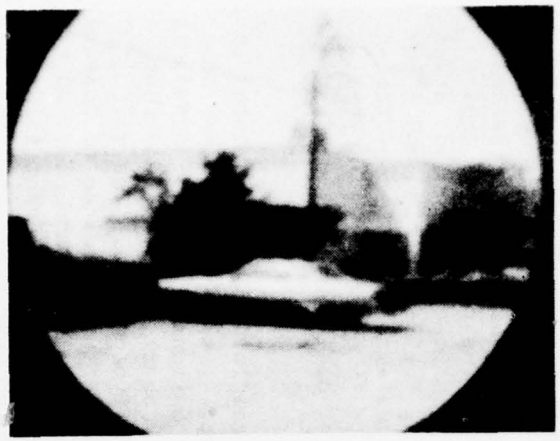

INCOHERENT, A = 1.4 mm

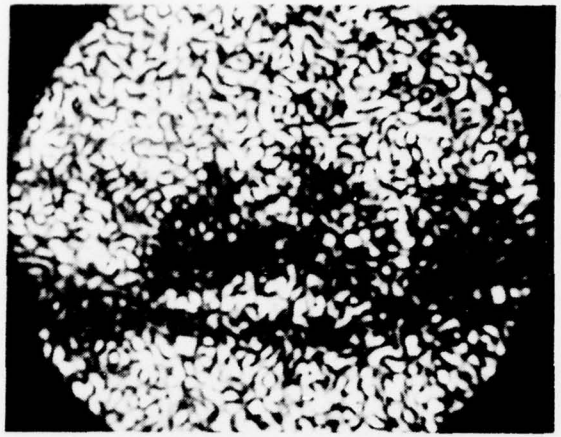

COHERENT, A = 1.4 mm

ORIGINAL TRANSPARENCY

Figure 1. Comparison of incoherent and coherent imaging at the same optical system resolution.

obtained using incoherent illumination and an estimate of the incoherent smoothing required to approach the performance of an incoherent system is made.

II. THE EXPERIMENTAL SYSTEM

The optical system used in the experiments is shown in Figure 2. The imaging system consists of two Jaegers cemented astronomical doublets, L_1 and L_2, of 128-mm aperture and 629-mm focal length, f, arranged in an afocal configuration with an aperture at F midway between the two lenses. In this arrangement, the object plane 0 is imaged with unity magnification at the image plane I and the aperture in the filter plane F is used to control the spatial frequency response of the imaging process. The aperture used is an iris with a circular aperture which can be varied in diameter from 0.9 mm to 20 mm; circular pinholes of 0.4 mm and 0.6 mm diameter are used when apertures smaller than 0.9 mm are required.

The diffuse illumination is supplied by an argon ion laser operating at a wavelength of 514.5 nm; a linearly polarized plane wave from the laser illuminates a stationary opal glass diffuser, D, placed just to the left of the plane 0. To conduct experiments using spatially incoherent illumination, an additional diffuser is placed between the light source and the stationary diffuser. This diffuser is moved continuously to simulate a spatially incoherent source. Because an opal glass diffuser depolarizes the laser light, a linear polarizer is placed just to the right of plane 0 to insure that only one component of the light field is used.

The object transparency, T, is placed in plane 0 and the image is observed in plane I using a microscope. The image is directly recorded by means of a 35-mm camera at plane I or, as an alternative, an auxiliary optical system is used to relay and magnify the plane I for recording of the image using a 4×5 Graflex back and Polaroid type 57 film. The optical system produces essentially diffraction limited images for an object field of over 2 cm diameter with resolutions well over 40 ℓ/mm.

III. GRATING IMAGING

An Ealing High Resolution Test Target was used to determine the effect of speckle on resolution in the imaging of periodic gratings. This target contains three groups of fifteen-bar high contrast targets where the spatial frequency ratio between successive targets is $10^{0.1}$. Only two groups are of interest because of the spatial frequency capability of the optical system. These two groups have spatial frequencies which vary from 1 to 10 ℓ/mm and 10 to 100 ℓ/mm, respectively. Over this range of spatial frequencies, the target very closely approximates a periodic square wave.

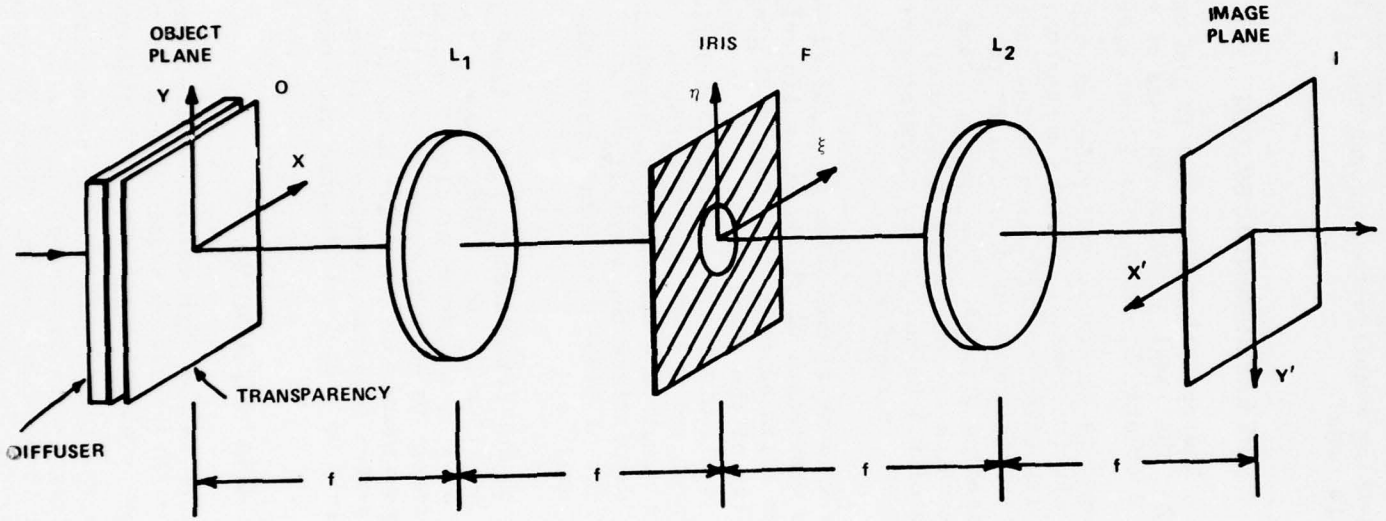

Figure 2. The optical system used in the experiments.

This object was imaged with spatially incoherent illumination through a series of apertures of diameters varying from 0.4 mm to 12.4 mm and each image was recorded on Polaroid film. The diameters were selected so that the spatial frequency response of the imaging system was just large enough to pass the fundamental frequency of one of the fifteen-bar target square waves. These data are shown in Figure 3 along the line marked INCOHERENT. Figure 4(a) is a photograph of the image produced with an aperture of 2.1 mm diameter. This photograph shows the 5.01 ℓ/mm target resolved at a very low contrast as would be expected when such a target is photographed with an aperture of cut-off frequency of approximately 5.3 ℓ/mm.

The object was imaged through the same apertures but spatially coherent illumination was used. Again, for each aperture, the image was recorded on Polaroid film and these photographs were used to determine which target could be resolved. Three observers judged the resolution by viewing the photographs from a distance sufficiently large so that the speckle superimposed on the grating was poorly resolved and thus appeared smoothed to the observer. The criterion used to judge the resolution was that a target was resolved if a relatively continuous grating structure existed over nearly the entire width of the grating target. These data are plotted along the line marked COHERENT in Figure 3. Figure 4(b) is a photograph taken through a 4.1-mm diameter aperture and shows the 5.01 ℓ/mm grating target which was judged to be resolved by the preceding criterion. From an examination of these data, it appears that the aperture of a coherently illuminated system must be twice as large as that of an equivalent incoherently illuminated system to achieve equal resolution. Figure 5 illustrates this point. This is the same conclusion which is reached based on a consideration of the spatial frequency bandwidths of the two types of systems independent of the type of object being imaged. However, it was felt that the presence of speckle in diffuse imaging should make the size of the aperture required larger than twice the incoherent aperture size and that the observer, in the act of judging the resolution, was providing some averaging of the speckle noise. This possibly was thought to exist because the grating target was considerably larger in width than the period of the grating.

The photographs produced in coherent illumination were then reexamined with an aim of eliminating the possibility of unconscious smoothing by the observer. A slit of width equal to the period of the grating was placed over the photograph and oriented perpendicular to the lines of the target. The grating structure was examined through this slit and the question of resolution was determined by judging whether a periodic structure could be discerned along the slit.

This effect can be seen in Figure 4(b) by placing a slit over the figure; with the slit in place the third target from the bottom (5.01 ℓ/mm) is not resolved while the fourth target from the bottom (3.92 ℓ/mm) is resolved. The data obtained in this way are shown along

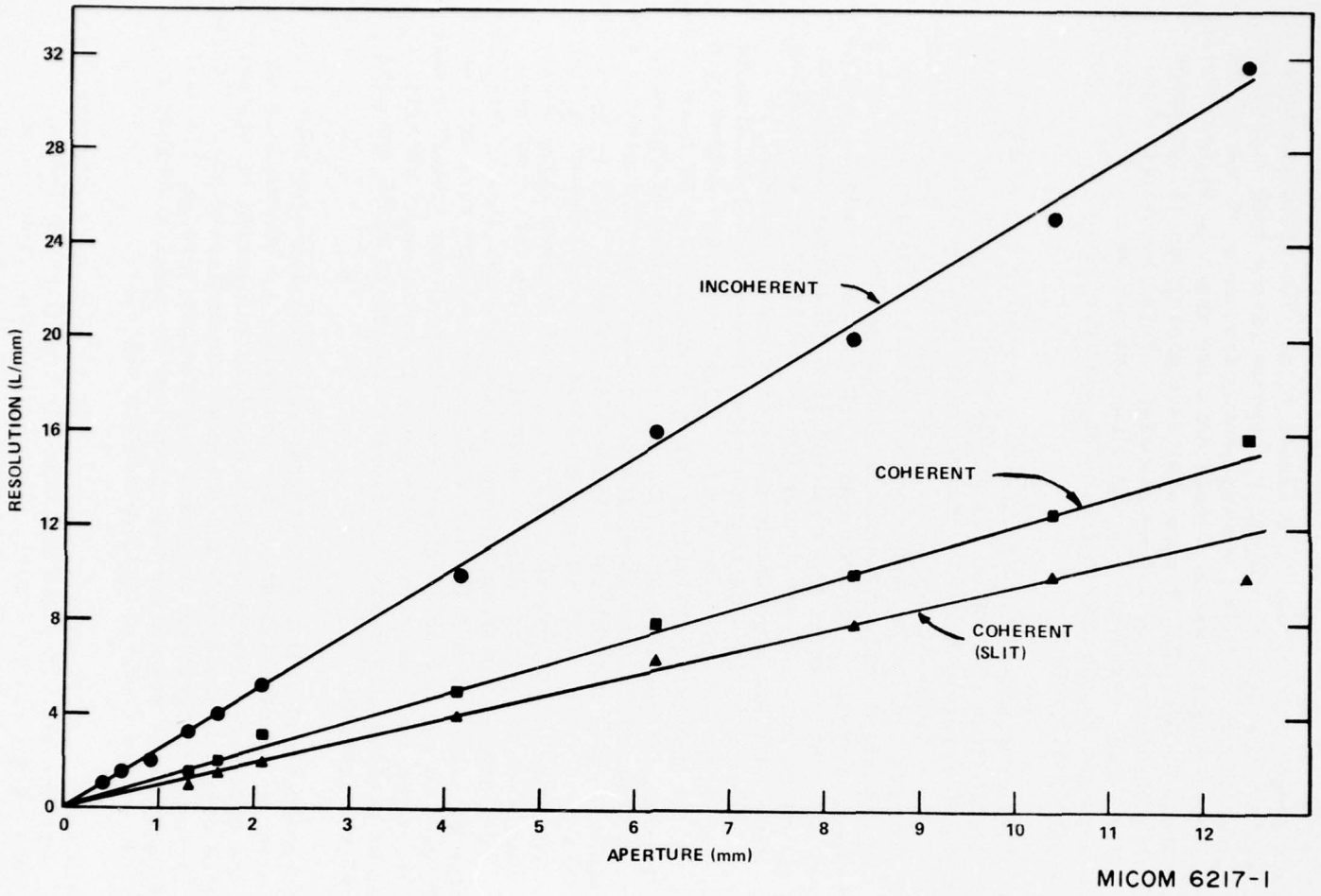

Figure 3. Resolution as a function of optical system aperture for (1) incoherent imaging, (2) coherent imaging with resolution judged by viewing the entire bar pattern, and (3) coherent imaging with resolution judged by viewing the bar pattern through a slit of width equal to the grating period.

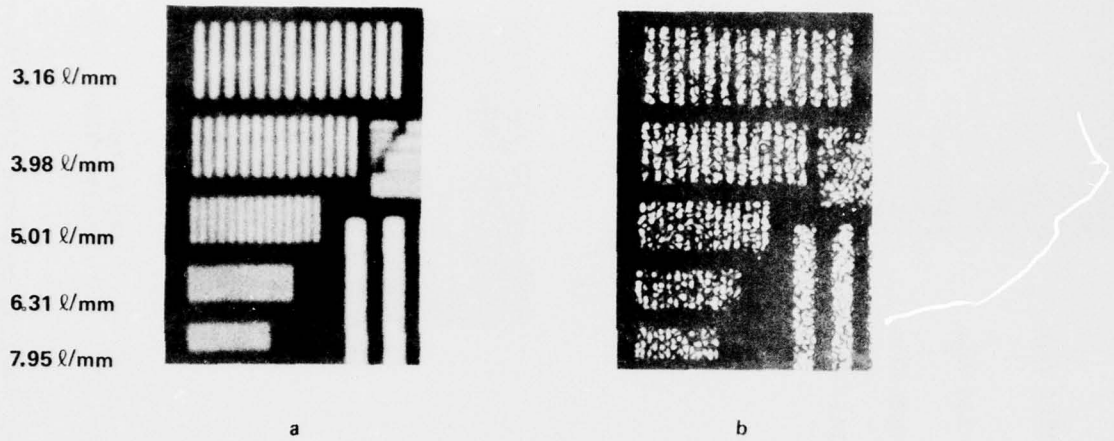

Figure 4. Bar targets imaged (a) incoherently with a 2.1-mm aperture, and (b) coherently with a 4.1-mm aperture.

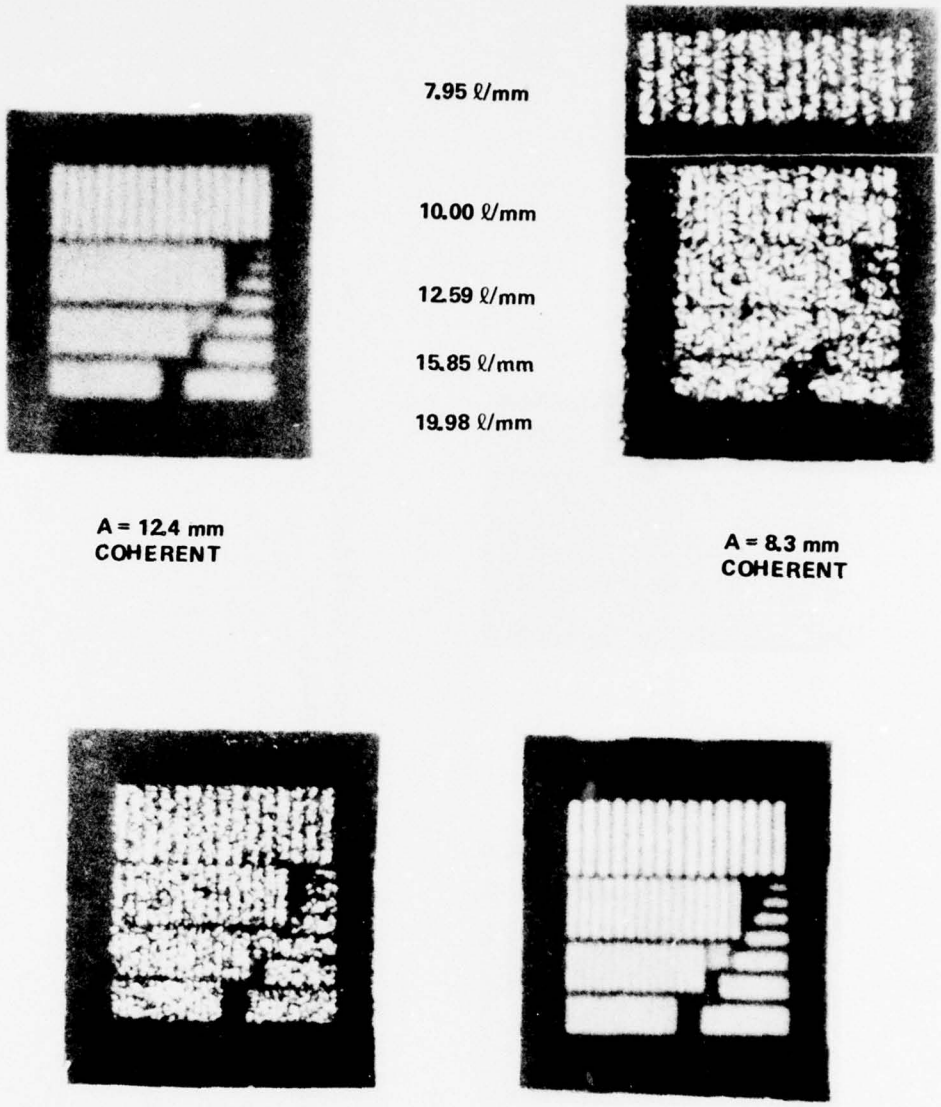

Figure 5. Incoherent bar target imaging compared with coherent bar target imaging with a factor of two greater system resolution.

the line marked COHERENT (SLIT) in Figure 3 and show that an increase of 2.6 in aperture diameter over an incoherent system is required to provide equal resolution in a system which images coherently illuminated diffuse gratings.

It is well known that the mean value to standard deviation ratio, m/σ, of a speckle pattern produced with coherent illumination is unity. It is also known that this signal-to-noise ratio, m/σ, can be increased by adding together independent speckle patterns; the increase in m/σ is equal to the $\sqrt{N}$ where N is the number of independent additions. To determine how resolution is affected by increasing the signal-to-noise ratio of the speckle pattern, the coherently illuminated diffuse grating target was smoothed in this way. A series of coherent images of the grating was produced; each was superimposed with an independent speckle pattern. Each of these images was made with the aperture of Figure 2 placed in a different position in plane F. To insure independence of the speckle patterns, the minimum distance between any two positions of the aperture was equal to or greater than the aperture diameter. The series of images produced in this way was recorded as equal increments of exposure on a Polaroid film. The results of this experiment are shown in Figures 6 and 7, where the number of independent speckle patterns which were added to produce each panel of the figure is given below the panel. The panel marked $N = \infty$ was produced using spatially incoherent illumination. The aperture used to produce these photographs was of a size required just to resolve the 3.98 ℓ/mm periodic target with spatially incoherent illumination. Figures 6 and 7 were used to determine the spatial frequencies of the bar targets just resolved by the slit criterion. These values of resolution are plotted as a function of N in Figure 8. It can be concluded from these data that the addition of approximately 100 uncorrelated speckle patterns, a signal-to-noise ratio of approximately 10, is required to approach the resolution performance of an incoherently illuminated system.

IV. CONTINUOUS TONE IMAGING

Determining the effect of speckle on resolution when imaging objects having a continuous spatial frequency distribution and range of contrasts is not as straightforward as it is with gratings because more subjective judgement is required to form conclusions. In an attempt to minimize the requirement for subjective judgement, a technique was devised in which an incoherent reference image was compared to a set of coherently produced images and to low-pass filtered versions of these coherently produced images.

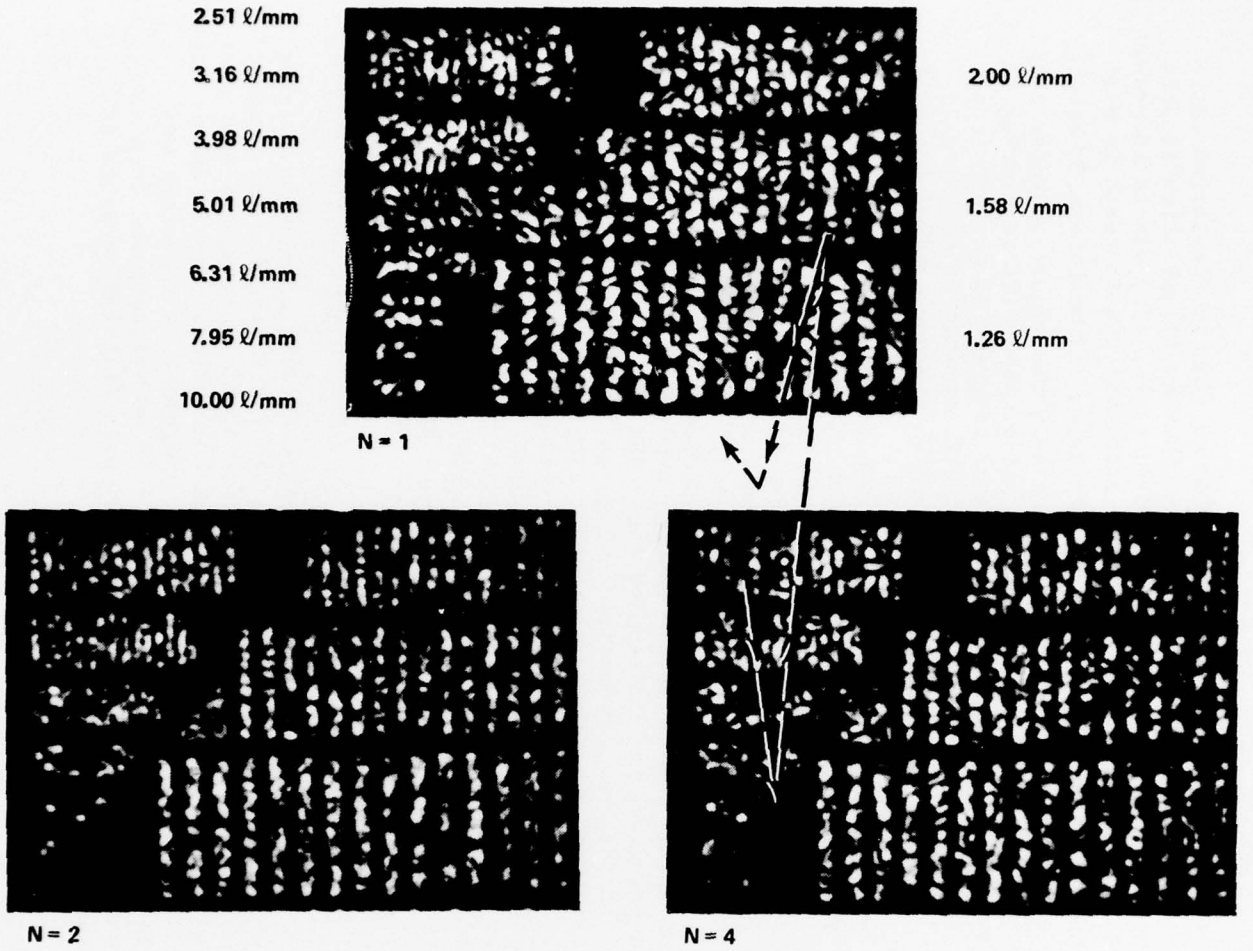

Figure 6. Increase in bar target resolution with the number, N, of superimposed coherent images with independent speckle patterns.

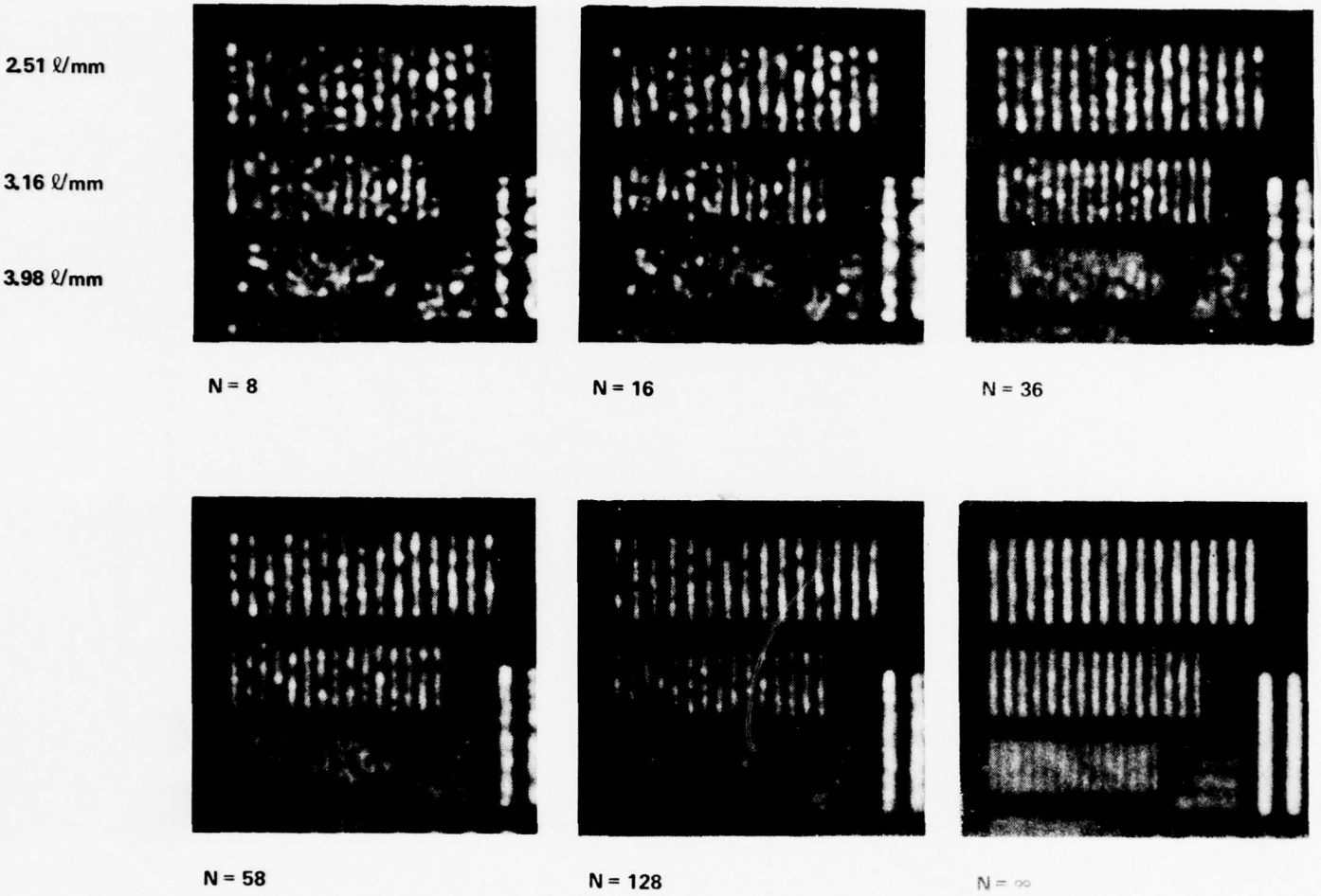

Figure 7. Increase in bar target resolution with the number N, of superimposed coherent images with independent speckle patterns. The image marked N = ∞ was produced using incoherent illumination.

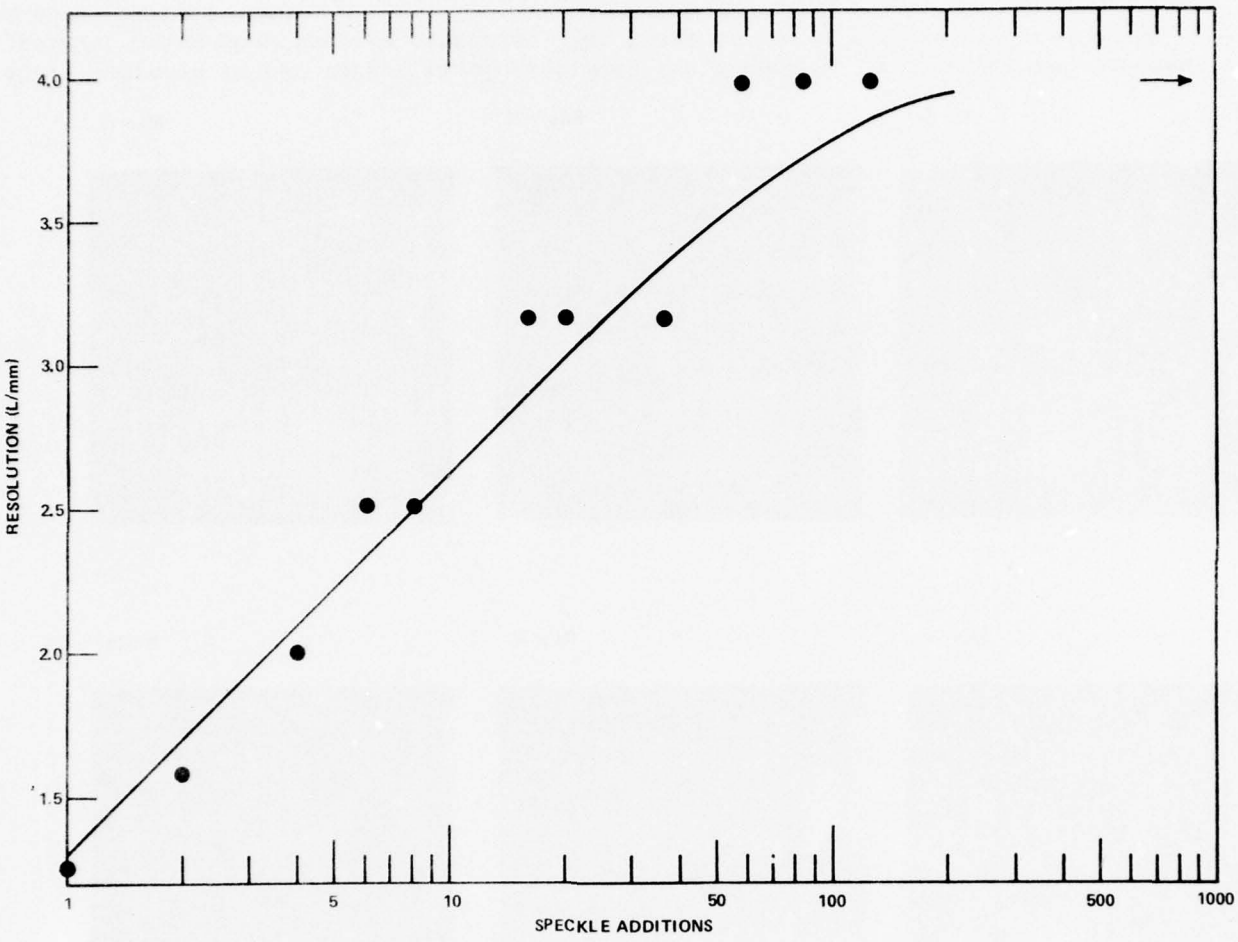

Figure 8. Bar target resolution, by slit criterion, as a function of the number of superimposed coherent images with independent speckle patterns.

The continuous tone object used for the experiment was an automobile. The object transparency of this automobile is shown in Figure 1. A reference image was prepared from the transparency using incoherent illumination in the optical system shown in Figure 2. The aperture used to prepare this reference image was 1.44 mm in diameter producing an image with approximately 6.4 lines of resolution across the height of the automobile in the foreground. This resolution, according to the Johnson criteria [7], is at the average identification level of object classification. The reference image is denoted "incoherent, A = 1.4 mm" in Figure 1 and Figures 9 through 14.

A set of images was then made using coherent illumination. These images were prepared with the optical system of Figure 1 by using a negative of the object transparency of the automobile and photographing the resultant image on 35-mm Panatomic-X film at the image plane I. A series of images were obtained using apertures of 12.4, 10.4, 8.3, 6.2, 4.1, and 2.1 mm in diameter. Photographs of these images are labeled "coherent" in Figures 9 through 14. The 35-mm transparencies produced in this coherently illuminated step were then placed in the object plane of the optical system and imaged at Plane I through a 1.44-mm diameter aperture using incoherent illumination. The process of forming these filtered coherent images is shown schematically in Figure 15. This low-pass filtering operation reduces the resolution of the coherently produced images to that of the reference image and increases the signal-to-noise ratio by smoothing the speckle, making the resulting photographs similar in appearance to the reference image. The images, recorded using Polaroid film through the auxiliary optical system, are labeled "coherent, filtered" in Figures 9 through 14. Because the resultant images have the same resolution as the incoherent, A = 1.4-mm reference image shown in Figures 9 through 14, a determination can be made of which images are of a quality comparable to the reference image by judging whether the detail present in the reference image can be discerned in a low-pass filtered image.

Examination of the results shows that the coherent, filtered images in Figures 9 and 10 are of comparable quality to the reference image while in the coherent, filtered images in Figures 11 through 14 there is a noticeable loss of some of the detail present in the reference image. These observations lead to the conclusion that for continuous tone objects the aperture of a coherently illuminated system must be increased by a factor of approximately seven over the aperture of an incoherent system to achieve equal performance.

It is shown in Appendix C that the signal-to-noise ratio of the low-pass filtered images of Figures 9 through 14 is given by the expression $m/\sigma = 1.48\ (D/d)$, where D is the diameter of the aperture used in the coherent imaging step while d is the diameter of the aperture used in the low-pass filtering process. This expression can be derived by using a model of the two-step imaging process given by Lewis [4] which considers the coherent and incoherent imaging steps

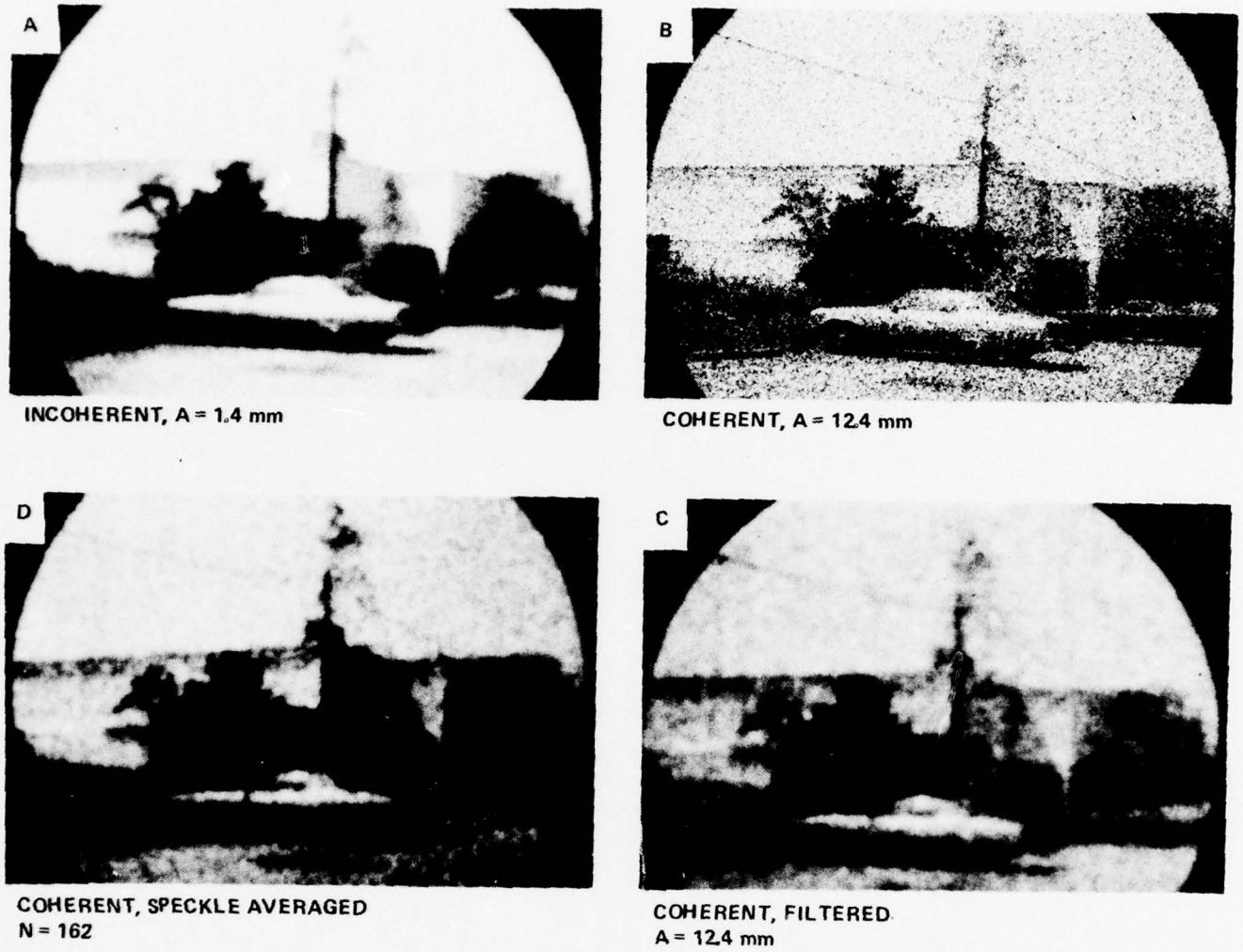

Figure 9. (a) Incoherent reference image for comparison with, (b) coherent image made at 8.6 times greater system resolution, (c) incoherently filtered coherent image, and (d) speckle averaged coherent image equivalent to the filtered image.

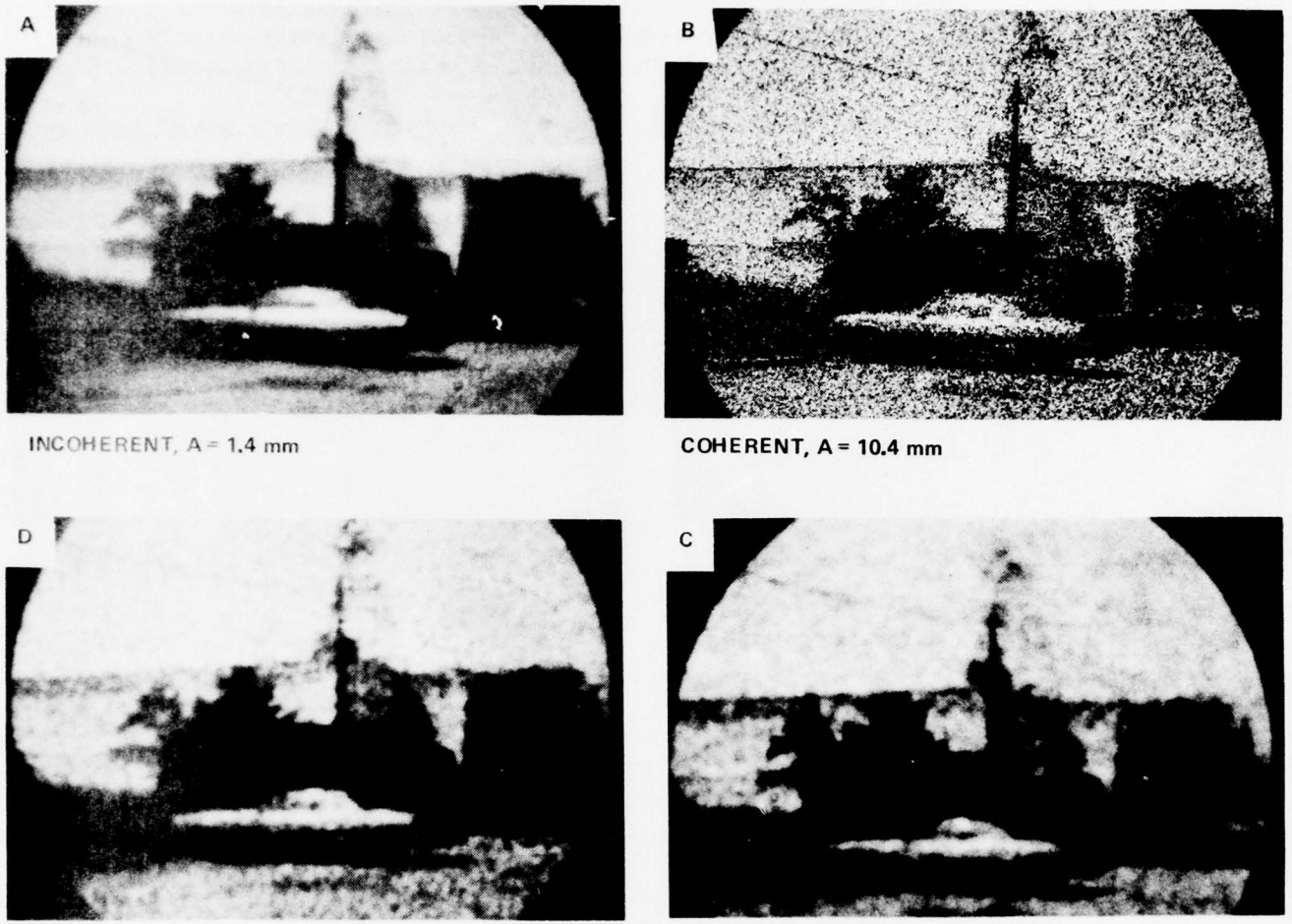

Figure 10. (a) Incoherent reference image for comparison with, (b) coherent image made at 7.2 times greater system resolution, (c) incoherently filtered coherent image, and (d) speckle averaged coherent image equivalent to the filtered image.

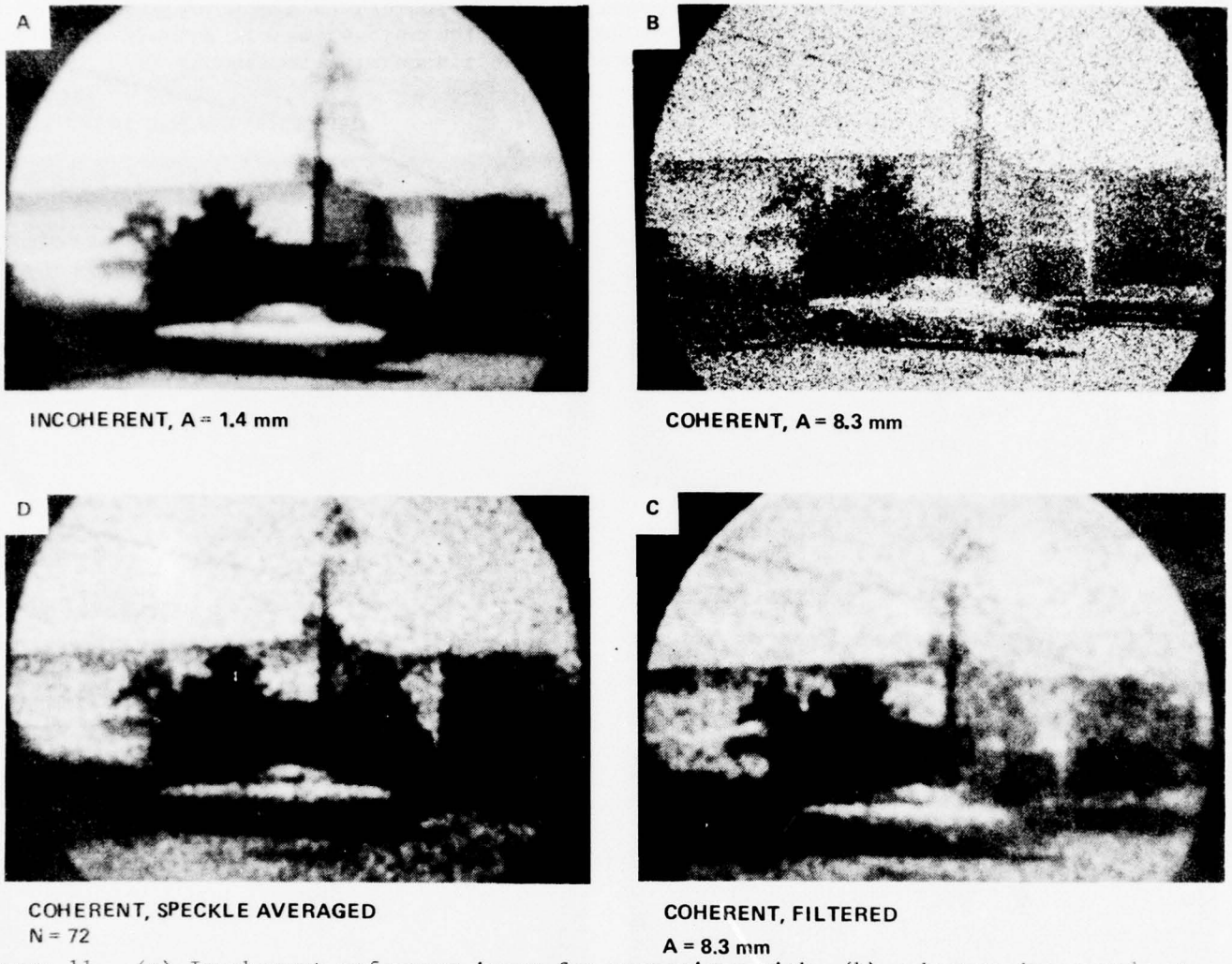

Figure 11. (a) Incoherent reference image for comparison with, (b) coherent image made at 5.8 times greater system resolution, (c) incoherently filtered coherent image, and (d) speckle averaged coherent image equivalent to the filtered image.

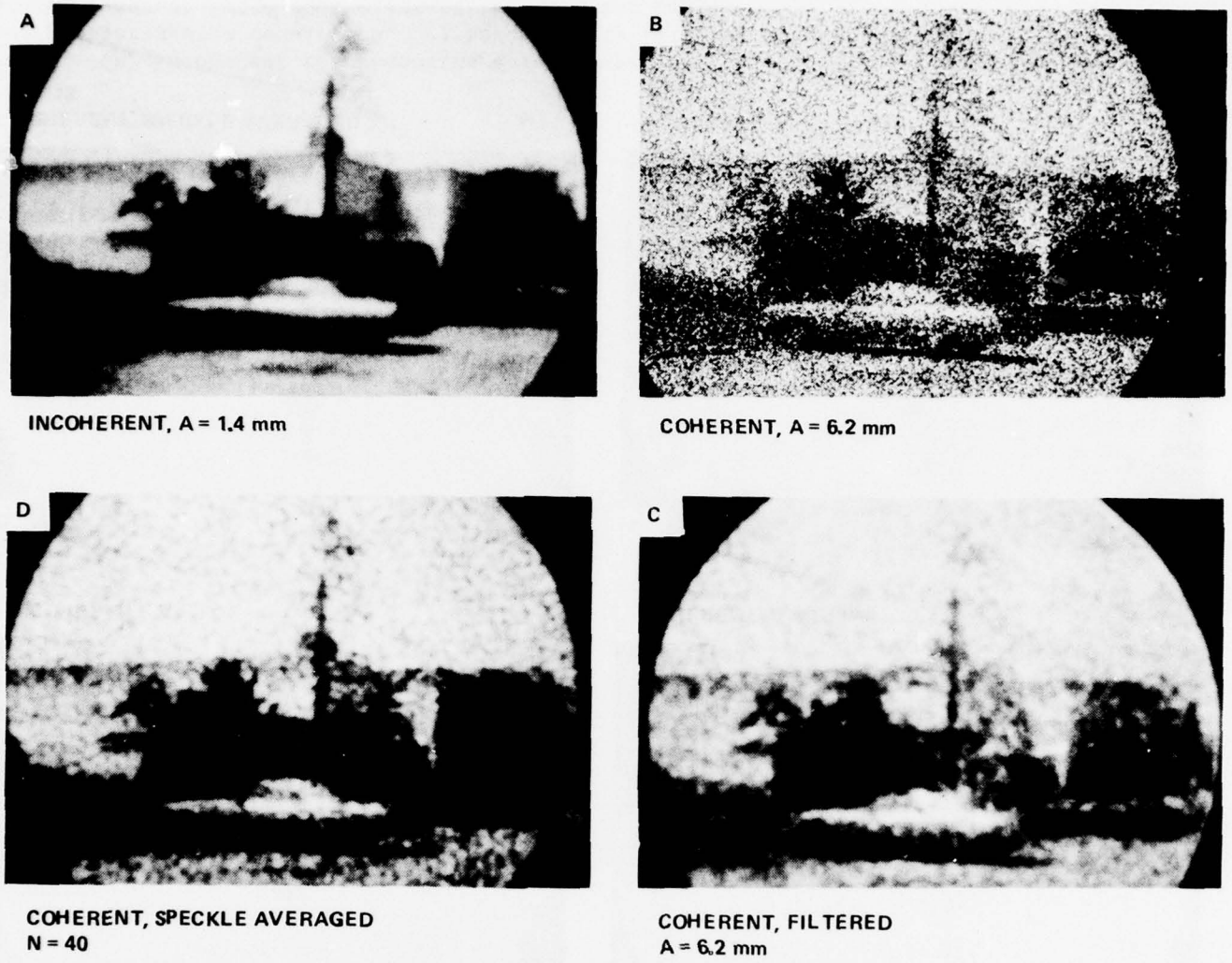

Figure 12. (a) Incoherent reference image for comparison with, (b) coherent image made at 4.3 times greater system resolution, (c) incoherently filtered coherent image, and (d) speckle averaged coherent image equivalent to the filtered image.

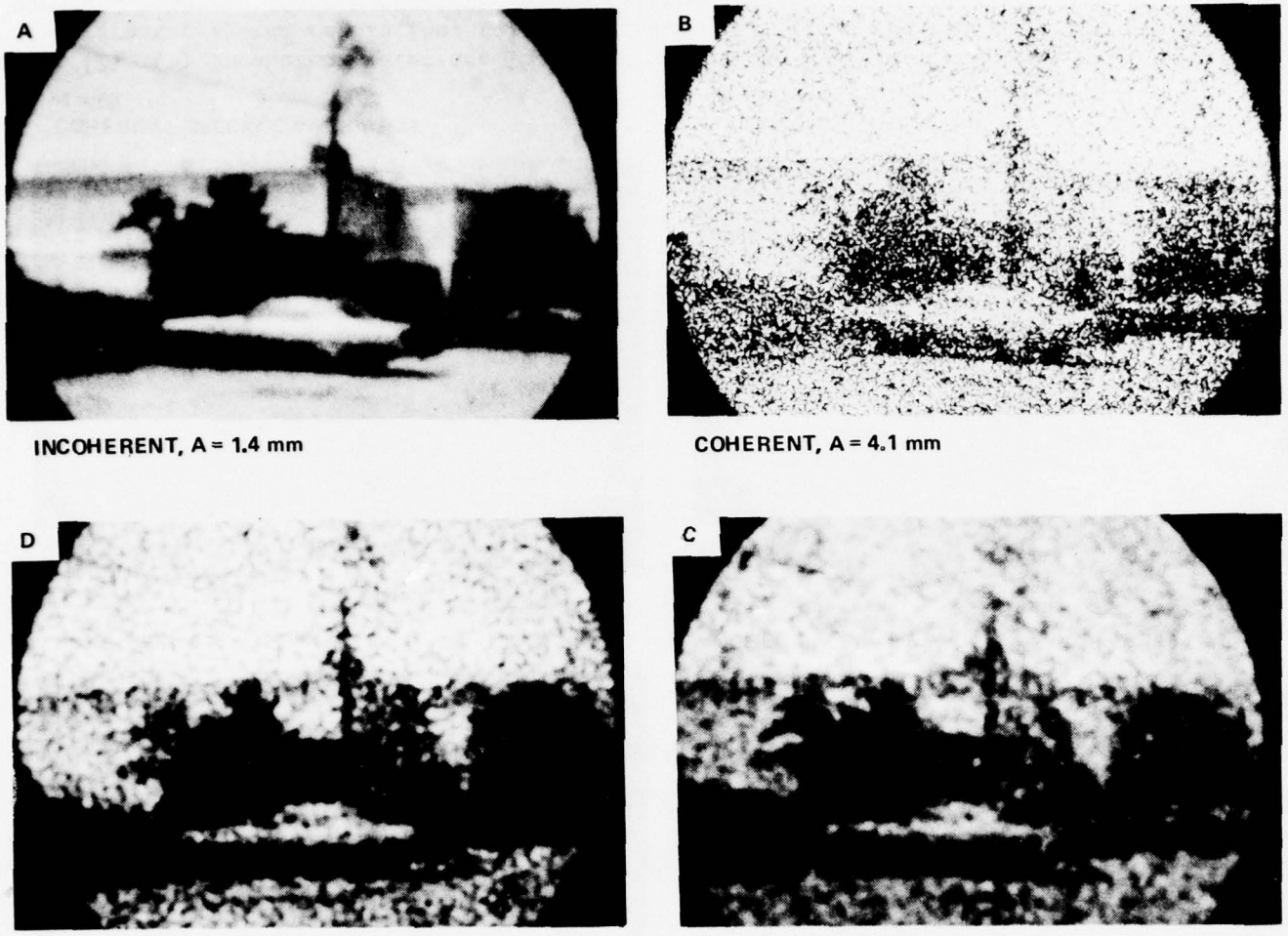

Figure 13. (a) Incoherent reference image for comparison with, (b) coherent image made at 2.8 times greater system resolution, (c) incoherently filtered coherent image, and (d) speckle averaged coherent image equivalent to the filtered image.

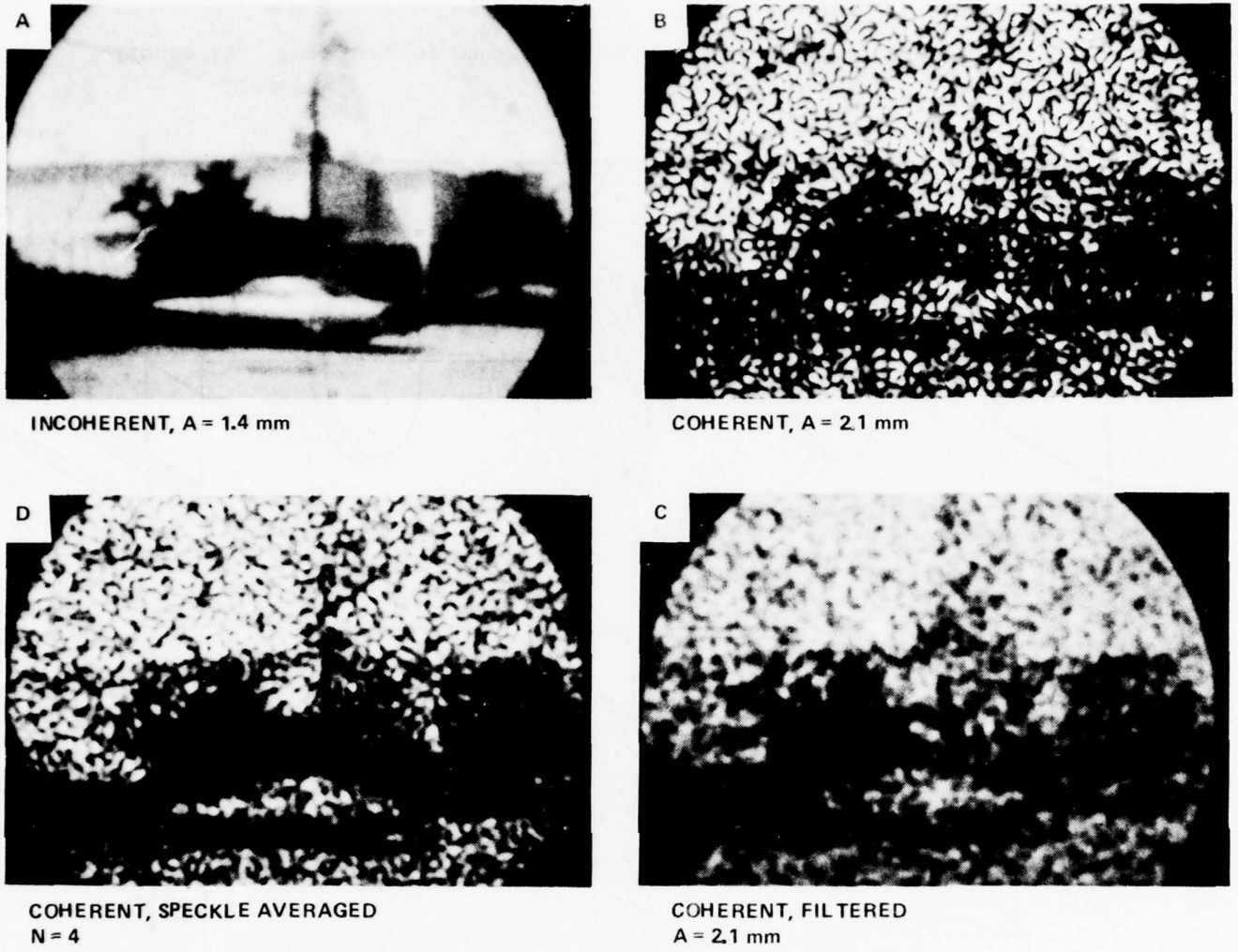

Figure 14. (a) Incoherent reference image for comparison with, (b) coherent image made at 1.5 times greater system resolution, (c) incoherently filtered coherent image, and (d) speckle averaged coherent image equivalent to the filtered image.

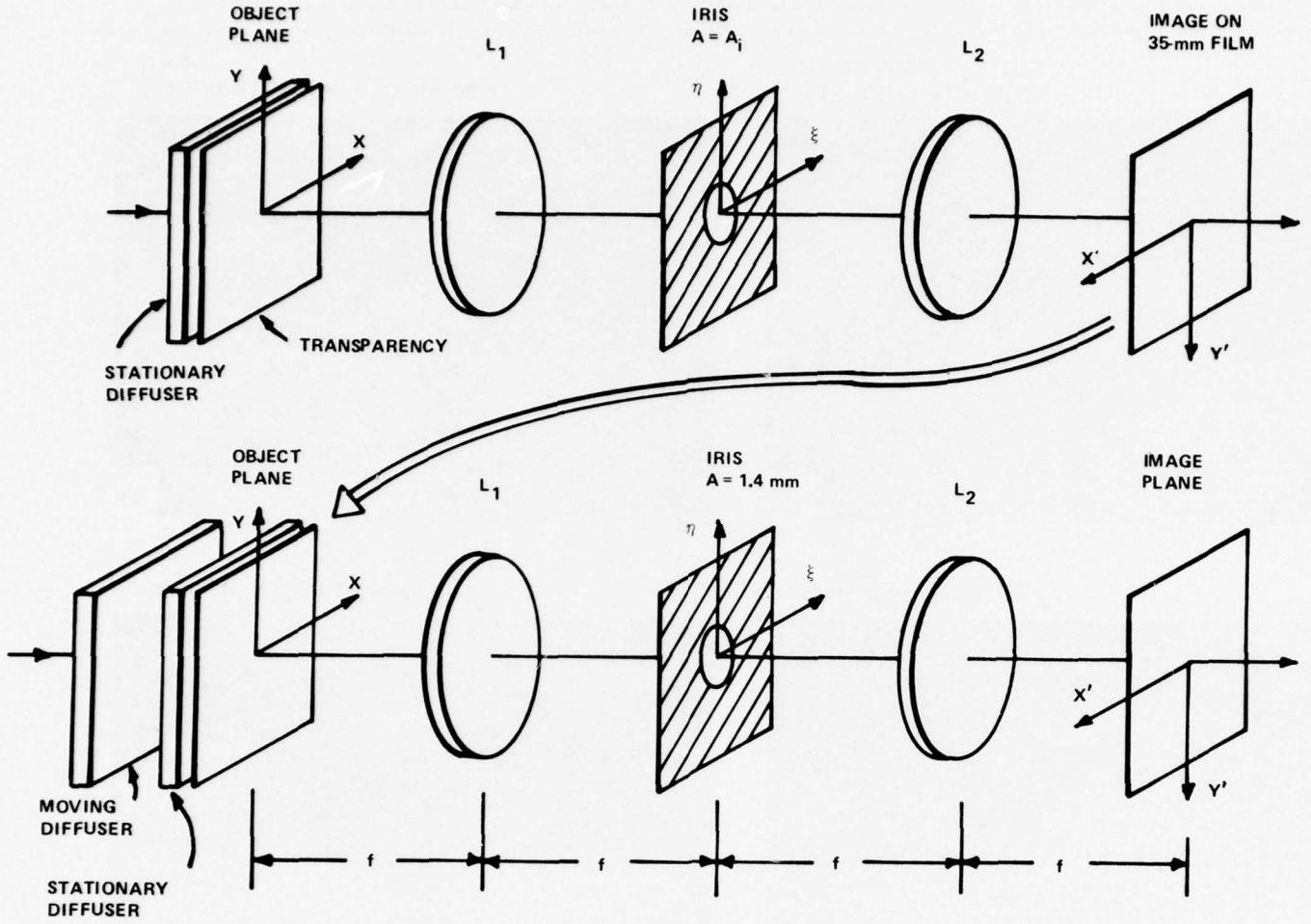

Figure 15. Smoothing of coherent images by incoherent filtering.

as linear filtering operations and the intermediate recording of the coherent image as a square law detection process. Using this expression to calculate m/σ for the coherent, filtered images in Figures 9 through 12, 12.7, 10.7, 8.5 and 6.4 respectively, are obtained. The signal-to-noise ratio for the filtered images in Figures 9 and 10, the images considered of comparable quality to the reference image, is ten or greater, while this ratio is less than 10 for the filtered images in Figures 11 and 12 which were judged to be of unacceptable quality. This result is similar to that obtained previously in the imaging of diffusely illuminated gratings.

By equating expressions for the signal-to-noise ratio for low-pass filtered images, $m/\sigma = 1.48\ (D/d)$, with that for images formed by superposition of N independent coherent images, $m/\sigma = \sqrt{N}$, it is found that these two speckle smoothing techniques are equivalent for $N = 2.18\ (D/d)^2$. This expression was used to calculate values of N corresponding to the ratios of the apertures D and d used in recording the coherent, filtered images in Figures 9 through 14. For each of these values of N, a series of superimposed coherent images was recorded on Polaroid film using the 1.4-mm aperture, d. For each exposure the aperture was moved a sufficiently large distance in the plane F to produce an independent speckle pattern. The coherent, speckle averaged images formed in this manner are shown in Figures 9 through 14 with the corresoonding coherent, filtered images. A visual comparison of these speckle averaged images with the adjacent filtered images in these figures shows that the signal-to-noise ratio, resolution, and appearance are comparable for each pair of images. This good agreement provides confirmation for the expression for m/σ derived in Appendix C. A comparison of the reference image, incoherent, A = 1.4 mm, with the coherent, speckle averaged images in Figures 9 through 14 shows that for N greater than approximately 100 (Figures 9 and 10), the images are of comparable quality. Therefore, for continuous tone objects, a coherent imaging system can obtain resolution equivalent to an incoherent imaging system with the same aperture by addition of approximately 100 images with uncorrelated speckle patterns.

The image comparison test used to obtain the aperture ratio of seven gives a result which may be too pessimistic. A direct examination of the coherent image in Figure 11 indicates that sufficient information is present in this image to judge it comparable to the reference image. Although the automobile is masked by the fine speckle pattern, an observer can learn to ignore the effect of this pattern and can identify sufficient detail in the image to be convinced that it is comparable to the reference image. Some observers who were shown the images thought that even Figure 12 contains sufficient detail to judge it comparable to the reference image. These observations lead to the conclusion that it is better to view a coherent image directly than to view a smoothed version of a coherent image because the aperture of the coherent system need be increased by only a factor of approximately five, rather than seven, over an incoherent system for comparable resolution performance.

A question which the data presented here elicits is why can a diffusely illuminated grating be resolved with a smaller aperture than a continuous tone object? Although the reason for which this apparently anomalous effect occurs is not fully understood, a possible answer can be proposed [8]. The grating is a simpler structure; it is basically one-dimensional and has a higher contrast than the continuous tone object. Also, in the case of the grating, the observers were asked only to determine if a periodic structure was present, whereas, in the case of the continuous tone object, they were asked to make a more complicated decision about whether as many details could be discerned in the image as in the reference image. Thus, it appears the observer may be able to make a decision about the grating with less information than is required for the continuous tone object. The complete answer to this question awaits a more detailed analytical and experimental investigation of resolution in the presence of speckle which is beyond the scope of the present study.

V. CONCLUSIONS

The effect of speckle in the imaging of diffusely illuminated gratings and continuous tone objects was studied. It was found that when imaging diffuse gratings, the aperture of a coherently illuminated system must be 2.6 times as large as that of an incoherent system to obtain comparable resolution. This factor must be increased to five when imaging objects with a continuous spatial frequency distribution and range of contrasts; it must be increased to a factor of seven if the coherent image is subsequently low-pass filtered. A coherent system can achieve resolution which is comparable to an incoherent system of equal aperture if the coherent image is smoothed so that the mean to standard deviation ratio of the speckle is ten or more.

Appendix A. SPECKLE WITH COHERENT SCANNED ILLUMINATION

Experiments were performed demonstrating speckle in images illuminated by a small spot of coherent light scanned over the object and a comparison made between the image speckle resulting from coherent flood illumination of the object with the speckle resulting from scanned illumination. An imaging system was assembled, similar to that shown in Figure 2 using an aperture in plane, F, to control resolution. The target consisted of a high contrast transmission bar chart in contact with a ground glass diffuser. A polarization analyzer was placed in the imaging system and oriented to pass only the component perpendicular to the polarization of the beam incident on the diffuser. The specular transmission through the diffuser was therefore blocked and high contrast speckles were obtained from the one polarization component passed. A HeNe laser operating at 6320Å was used for illumination and photographs were made at f/40.

Images of the 10.00, 7.95, 6.31, and 5.01 ℓ/mm groups and a part of the 1.26 ℓ mm group of the test target are shown in Figure A. The photograph labeled "not scanned" shows the bar chart illuminated with a uniform coherent beam covering the entire chart. The two photographs at the bottom of the figure were recorded by scanning an illuminating spot over the bar chart in a raster. The scanning spot size was made the same as the imaging system resolution spot size to match the practical requirements for long wavelength, active imaging systems. The photograph on the lower left shows the results when the raster scan lines overlap. In the photograph in the lower right-hand side of Figure A, the scan lines were separated to show the raster.

The speckle is expected to be similar in both the flood illuminated case and the scan illuminated case; this is shown in Figure A. Only that part of the diffuser within the optical system resolution spot on the object contributes to the speckle in the image. This is quite different from the nonimaging case in which each point illuminated on the object scatters light to every point on the observation plane. Light scattered at points on the object separated by a few resolution spot diameters will be imaged independently on the image plane although some overlap of point spread functions occurs. As a first approximation, light imaged at adjacent resolution spots on the image arises from independent ensembles of scatterers at the corresponding spots on the object. Therefore, the speckle at each point on the image arises from the same ensemble of scatterers on the object if the entire object is illuminated simultaneously or point-by-point with a scanning spot. For a sufficiently fine grained diffuser as an object, i.e., a large number of scattering points within the resolution spot, the speckle size, ℓ, depends only on the imaging system limiting aperture, D, the focal length, F, and the illumination wavelength λ:

$$\ell \approx \frac{\lambda f}{D} \quad . \tag{A-1}$$

NOT SCANNED

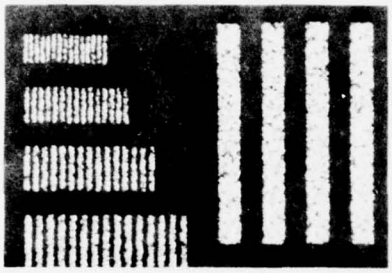

OVERLAPPING SCAN LINES

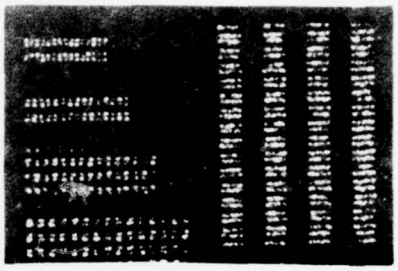

NONOVERLAPPING SCAN LINES

Figure A. Speckle with coherent scanned illumination. The scanning spot size is the same as the camera resolution.

The similarity of the speckle for the two types of illumination shown in Figure A-1 confirm the validity of this simple model.

Some decrease in speckle contrast is observed in the scanned illumination case due to second-order effects such as speckle averaging. The entire camera resolution spot is not fully illuminated during much of the time the illumination spot is scanned over it. Therefore, the film records a superposition of the speckle pattern resulting from illumination of the entire spot and the patterns resulting from illumination of parts of the spot. The large amount of overlap in illumination as a resolution spot is scanned leads to a large amount of correlation between instantaneous patterns and the decrease in contrast from averaging is less than for independent patterns.

Appendix B. SPECKLE AVERAGING TECHNIQUES

Speckle averaging by superposition of coherent images with uncorrelated speckle patterns was discussed previously in this report. In order to decorrelate the speckle, it was found to be convenient to move the aperture of Figure 2 to N positions in plane F that are separated by a distance greater than or equal to the aperture diameter. However, other techniques can also be used.

For the thick opal glass diffusers used in these experiments, the transmitted light is depolarized and the parallel and crossed polarized components yield images with uncorrelated speckle patterns [9]. Therefore, an image formed without an analyzer in the optical system corresponds to the addition of two coherent images with independent speckle patterns.

Speckle patterns formed when the diffuser is illuminated at sufficiently different wavelengths are also decorrelated [3]. The wavelength separation required is dependent on the diffuser characteristics. For the thick opal glass diffusers used in this work, a separation of 15Å is adequate [10]. Therefore, speckle reduction can be obtained by adding coherent images formed at a number of different illumination wavelengths.

The equivalence of polarization diversity and frequency diversity for speckle reduction is demonstrated in Figure B-1. Figure B-2 illustrates the equivalence between frequency diversity and angular diversity (displacing the aperture in plane F of Figure 2). Note that the signal-to-noise ratio and resolution appear to be the same for pairs of images formed by superimposing the same number of coherent images with the speckle decorrelated by these three different techniques.

Appendix B. SPECKLE AVERAGING TECHNIQUES

Speckle averaging by superposition of coherent images with uncorrelated speckle patterns was discussed previously in this report. In order to decorrelate the speckle, it was found to be convenient to move the aperture of Figure 2 to N positions in plane F that are separated by a distance greater than or equal to the aperture diameter. However, other techniques can also be used.

For the thick opal glass diffusers used in these experiments, the transmitted light is depolarized and the parallel and crossed polarized components yield images with uncorrelated speckle patterns [9]. Therefore, an image formed without an analyzer in the optical system corresponds to the addition of two coherent images with independent speckle patterns.

Speckle patterns formed when the diffuser is illuminated at sufficiently different wavelengths are also decorrelated [3]. The wavelength separation required is dependent on the diffuser characteristics. For the thick opal glass diffusers used in this work, a separation of 15Å is adequate [10]. Therefore, speckle reduction can be obtained by adding coherent images formed at a number of different illumination wavelengths.

The equivalence of polarization diversity and frequency diversity for speckle reduction is demonstrated in Figure B-1. Figure B-2 illustrates the equivalence between frequency diversity and angular diversity (displacing the aperture in plane F of Figure 2). Note that the signal-to-noise ratio and resolution appear to be the same for pairs of images formed by superimposing the same number of coherent images with the speckle decorrelated by these three different techniques.

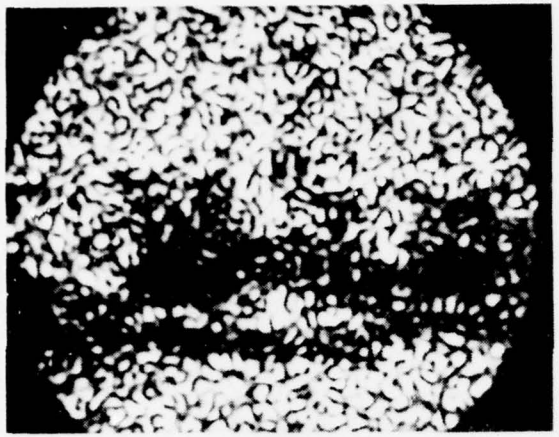

514.5 nm VERTICAL POLARIZATION

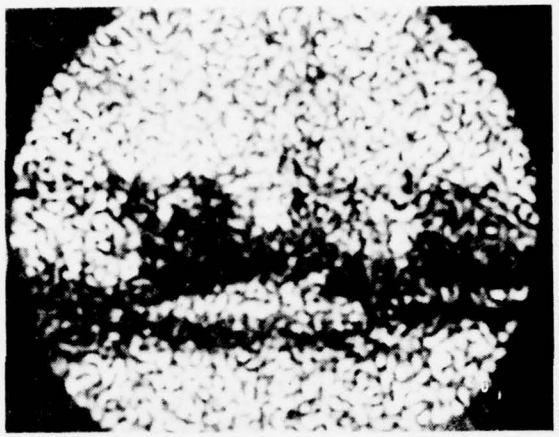

514.5 nm, VERTICAL AND
HORIZONTAL POLARIZATION

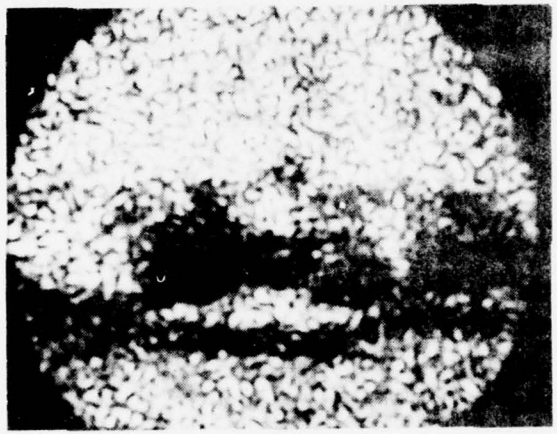

2 EXPOSURES, 514.5 nm AND 488.0 nm,
VERTICAL POLARIZATION

Figure B-1. Equivalence of frequency diversity and polarization diversity for speckle reduction.

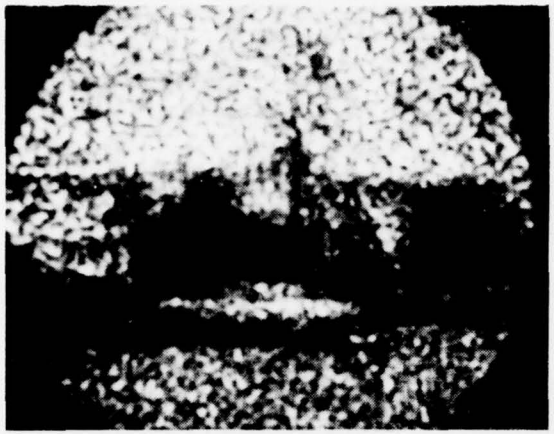

4 EXPOSURES, 514.5 nm, 501.7 nm, 488.0 nm AND 476.5 nm, VERTICAL POLARIZATION

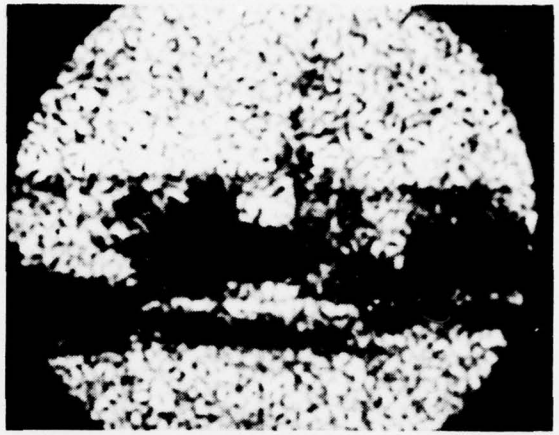

2 EXPOSURES, 2 POLARIZATIONS, APERTURE DISPLACED BETWEEN EXPOSURES

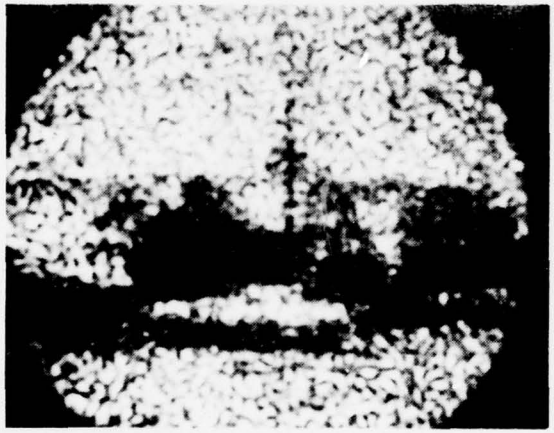

6 EXPOSURES, 514.5 nm, 501.7 nm, 488.0 nm, 476.5 nm, 465.8 nm, AND 454.5 nm, VERTICAL POLARIZATION

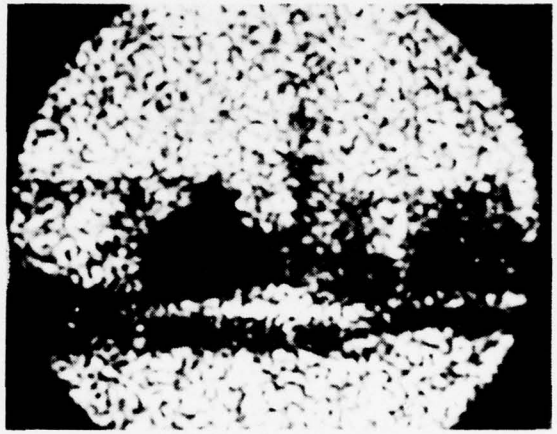

3 EXPOSURES, 2 POLARIZATIONS, APERTURE DISPLACED BETWEEN EXPOSURES

Figure B-2. Equivalence of frequency diversity and angular diversity for speckle reduction.

Appendix C. SIGNAL–TO–NOISE RATIO FOR LOW–PASS FILTERED COHERENT IMAGES

Incoherent filtering of coherent images is performed using the technique shown schematically in Figure 15. A primary photographic transparency, T_1, is placed in the object plane x-y. A stationary diffuser is placed behind the transparency and a monochromatic plane wave from a laser is used to illuminate the diffuser and transparency in the object plane. Lenses L_1 and L_2, which are of equal focal length, are arranged as an afocal system and used to image the object plane x-y into an image plane x'-y' with unity magnification. An aperture, placed midway between lenses L_1 and L_2, is used to filter the image to control the resulting resolution captured at x'-y' on a camera. This intermediate image is developed and used for further processing.

After development of the image recorded at x'-y' as described previously, the resulting intermediate transparency, T_2, is placed back in the object plane x-y where it replaces the original transparency. The intermediate transparency is illuminated with a monochromatic plane wave which is further diffused by a moving ground glass to simulate spatially incoherent light. This spatially incoherent object is imaged by the afocal system through the filter into plane x'-y' where the final image is recorded. The resolution of this final image is controlled by the size of the filter placed midway between lenses L_1-L_2 as before.

The compound imaging process described can be modeled by the following system diagram.

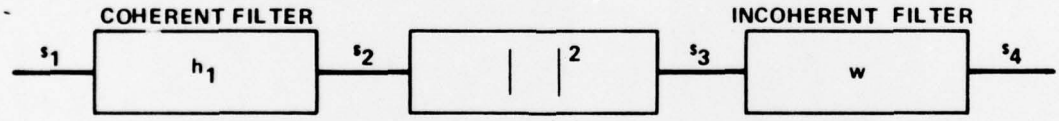

Figure C. System model.

The input s_1 represents the amplitude transmittance of the combination of the transparency T_1 and the stationary diffuser. The coherent filter with impulse response h_1 represents the filtering action of the aperture used in making the coherent intermediate transparency T_2. The block indicating the process of performing the magnitude squared operation approximately represents recording the complex amplitude of the coherent image on photographic film. The incoherent filter with impulse response w represents the combined action of the moving diffuser and the filtering action of the aperture placed at the midpoint of the afocal

system in the second imaging process. It can be shown that $w = |h_2|^2$ where h_2 is the coherent impulse response of the filter. That is, $W = H_2 * H_2^*$ where W and H_2 are the incoherent and coherent transfer functions, respectively, of the filter, * is the convolution operator and * is the conjugation operator. The signals s_1, s_2, s_3, s_4, are assumed to be functions of the two-dimensional space coordinates of the optical system. The input signal, s_1, is the complex amplitude of the light field existing just to the right of the transparency T_1 while the signal, s_2, is the complex amplitude of the image to be recorded after the first imaging process. It is assumed that the recording process captures the squared magnitude of s_2 linearly and produces an intensity transmittance such that the illuminance s_3 produced just to the right of the transparency T_2 in the second imaging process is proportional to $|s_2|^2$. The output signal s_4 is the luminance distribution of the image produced in the incoherent filtering process. This luminance produces the output image to be evaluated here. The criterion chosen for evaluation is the ratio of the mean squared value of the luminance to the variance of the luminance of the output light distribution s_4. A value is to be found for this ratio which depends upon the input signal s_1 and the impulse responses of the coherent and the incoherent filters. In order to proceed, it is assumed that s_1 is a complex valued Gaussian random process which is stationary and whose real and imaginary parts have mean value zero.

The calculation of the ratio proceeds as follows. The mean squared value of s_4 is by definition

$$m_{s_4}^2 = [E\{s_4\}]^2 \quad ,$$

where E(x) is used to indicate a statistical average. The signal s_4 is obtained by passing s_3 throughthe filter with impulse response w. Thus,

$$s_4 = s_3 * w = \iint_{-\infty}^{-\infty} s_3(x-x',y-y')\, w(x',y')\, dx'\, dy'$$

where * is the convolution operator. Performing the indicated averaging operation, the following equation is obtained:

$$m_{s_4} = E[s_4] = m_{s_3} \iint_{-\infty}^{\infty} w(x',y')\, dx'\, dy' = m_{s_3}\, W(0,0) \qquad \text{(C-1)}$$

because the transfer function, W, is obtained by taking a Fourier transform of the impulse response, w, as indicated below.

$$W(\xi,\eta) = \iint_{-\infty}^{\infty} w(x,y) e^{-j2\pi(\xi x+\eta y)}\, dx\, dy \quad .$$

The mean value of s_3 can also be expressed in terms of the autocorrelation function of s_2 evaluated at the origin as

$$m_{s_3} = R_{s_2}(0,0)$$

because by definition

$$R_{s_2}(\alpha,\beta) = E[s_2(\alpha-x,\beta-y)\ s_2{}^*(x,y)]$$

and

$$s_3(x,y) = |s_2(x,y)|^2 = s_2(x,y)\ s_2{}^*(x,y) \quad .$$

The spectrum of s_2, namely $S_{s_2}(\xi,\eta)$, can be written in terms of the spectrum of s_1 and the transfer function of the coherent filter because

$$S_{s_2}(\xi,\eta) = S_{s_1}(\xi,\eta)\ |H_1(\xi,\eta)|^2 \quad ;$$

thus

$$R_{s_2}(0,0) = \iint_{-\infty}^{\infty} S_{s_2}(\xi,\eta)\, d\xi\, d\eta = m_{s_3}$$

$$m_{s_3} = \iint_{-\infty}^{\infty} S_{s_1}(\xi,\eta)\ |H_1(\xi,\eta)|^2\, d\xi\, d\eta \quad . \qquad \text{(C-2)}$$

The transfer function of the incoherent filter can be written in terms of the coherent transfer function H_2 as

$$W(\xi,\eta) = H_2(\xi,\eta) * H_2^*(\xi,\eta)$$

or

$$W(\xi,\eta) = \iint_{-\infty}^{\infty} H_2(\xi-\xi',\eta-\eta')\, H_2^*(\xi',\eta')\, d\xi'\, d\eta' \quad ;$$

thus,

$$W(0,0) = \iint_{-\infty}^{\infty} |H_2(\xi,\eta)|^2\, d\xi\, d\eta \quad . \tag{C-3}$$

Combining Equations (C-1), (C-2), and (C-3), the mean value of s_4 is given by the expression

$$m_{s_4} = \left(\iint_{-\infty}^{\infty} S_{s_1}(\xi,\eta)\, |H_1(\xi,\eta)|^2\, d\xi\, d\eta\right)\left(\iint_{-\infty}^{\infty} |H_2(\xi,\eta)|^2\, d\xi\, d\eta\right) . \tag{C-4}$$

The variance of s_4 is by definition

$$\sigma_{s_4}^2 = E\{s_4^2\} - (E\{s_4\})^2 \quad . \tag{C-5}$$

To calculate the preceding equation, it is convenient to find the autocorrelation of s_3. This is defined as

$$R_{s_3}(\alpha,\beta) = E[s_3(x+\alpha,Y+\beta)\; s_3(x,y)] \quad .$$

Using the relation $s_3 = |s_2|^2$, this quantity can be written as

$$R_{s_3}(\alpha,\beta) = E[s_2(x+\alpha,y+\beta)\; s_2^*(x+\alpha,y+\beta) s_2(x,y)\; s_2^*(x,y)] \quad . \tag{C-6}$$

The signal s_2 is the result of passing the signal s_1 through a linear filter. Thus, both s_1 and s_2 are stationary complex Gaussian random processes; hence, Equation C-6 can be expanded by using the following theorem [11]:

$$E[x_1x_2x_3x_4] = E[x_1x_2]\ E[x_3x_4] + E[x_1x_3]\ E[x_2x_4] + E[x_1x_4]\ E[x_2x_3] \quad .$$

Thus, Equation (C-6) can be written as

$$R_{s_3}(\alpha,\beta) = E[s_2(x+\alpha,y+\beta)\ s_2^*(x+\alpha,y+\beta)]\ E[s_2(x,y)\ s_2^*(x,y)]$$

$$+ E[s_2(x+\alpha,y+\beta)\ s_2(x,y)]\ E[s_2^*(x+\alpha,y+\beta)\ s_2^*(x,y)]$$

$$+ E[s_2(x+\alpha,y+\beta)\ s_2^*(x,y)]\ E[s_2^*(x+\alpha,y+\beta)\ s_2(x,y)] \quad .$$

Because s_2 is stationary, the second term vanishes and the first and third terms become

$$R_{s_3}(\alpha,\beta) = \left\{ E[|s_2(x,y)|^2] \right\}^2 + R_{s_2}(\alpha,\beta)\ R_{s_3}^*(\alpha,\beta)$$

or

$$R_{s_3}(\alpha,\beta) = R_{s_2}^2(0,0) + |R_{s_2}(\alpha,\beta)|^2$$

The spectrum of s_3 is the Fourier transform of the autocorrelation function $R_{s_3}(\alpha,\beta)$. Thus,

$$S_{s_3}(\xi,\eta) = R_{s_2}^2(0,0)\ \delta(\xi,\eta) + S_{s_2}(\xi,\eta) * S_{s_2}(-\xi,-\eta) \quad , \qquad (C\text{-}7)$$

where $\delta(x)$ is the Dirac delta function. Returning to Equation (C-5), this equation can be expended by using Equations (C-1) and (C-2) and the relationships

$$E\{s_4^2\} = \int_{-\infty}^{\infty}\int S_{s_4}(\xi,\eta)\ d\xi\ d\eta$$

and

$$S_{s_4}(\xi,\eta) = S_{s_3}(\xi,\eta) \; |W(\xi,\eta)|^2$$

to obtain

$$\sigma_{s_4}^2 = \int_{-\infty}^{\infty}\int S_{s_3}(\xi,\eta) \; |W(\xi,\eta)|^2 \, d\xi \, d\eta - \left[W(0,0) \; R_{s_2}(0,0)\right]^2 \quad . \qquad \text{(C-8)}$$

By substituting Equation (C-7) into Equation (C-8), the following is obtained:

$$\sigma_{s_4}^2 = \int_{-\infty}^{\infty}\int \left\{R_{s_2}^2(0,0) \; \delta(\xi,\eta) + S_{s_2}(\xi,\eta) * S_{s_2}(-\xi,-\eta)\right\} |W(\xi,\eta)|^2 d\xi \, d\eta$$

$$- \left[W(0,0) \; R_{s_2}(0,0)\right]^2 \quad .$$

By integrating the first term, the result is

$$\sigma_{s_4}^2 = R_{s_2}^2(0,0) \; |W(0,0)|^2 + \int_{-\infty}^{\infty}\int \left\{S_{s_2}(\xi,\eta) * S_{s_2}(-\xi,-\eta)\right\} |W(\xi,\eta)|_2 \, d\xi \, d\eta$$

$$- W^2(0,0) \; R_{s_2}^2(0,0) \quad ,$$

which reduces to

$$\sigma_{s_4}^2 = \int_{-\infty}^{\infty}\int \left\{S_{s_2}(\xi,\eta) * S_{s_2}(-\xi,-\eta)\right\} |W(\xi,\eta)|^2 \, d\xi \, d\eta \quad . \qquad \text{(C-9)}$$

By noting that

$$S_{s_2}(\xi,\eta) = S_{s_1}(\xi,\eta) \; |H_1(\xi,\eta)|^2$$

and that

$$W(\xi,\eta) = H_2(\xi,\eta) * H_2(\xi,\eta) \quad ,$$

the following is obtained:

$$\sigma_{s_4}^2 = \iint_{-\infty}^{\infty} \left\{ S_{s_1}(\xi,\eta) \left|H_1(\xi,\eta)\right|^2 * S_{s_1}(-\xi,-\eta) \left|H_1(-\xi,-\eta)\right|^2 \right\} \left|H_2(\xi,\eta) * H_2(\xi,\eta)\right|^2 \, d\xi \, d\eta \quad . \tag{C-10}$$

To calculate the mean square to variance ratio of the output image Equations (C-4) and (C-10) can be combined to obtain

$$\frac{m_{s_4}^2}{\sigma_{s_4}^2} = \frac{\left(\iint_{-\infty}^{\infty} S_{s_1}(\xi,\eta) \left|H_1(\xi,\eta)\right|^2 d\xi \, d\eta \right)^2 \left(\iint_{-\infty}^{\infty} \left|H_2(\xi,\eta)\right|^2 d\xi \, d\eta \right)^2}{\iint_{-\infty}^{\infty} \left\{ S_{s_1}(\xi,\eta) \left|H_1(\xi,\eta)\right|^2 * S_{s_1}(-\xi,-\eta) \left|H_1(-\xi,-\eta)\right| \right\}^2 \left|H_2(\xi,\eta) * H_2(\xi,\eta)\right|^2 d\xi \, d\eta} \tag{C-11}$$

If it is assumed that the spectrum of s_1 is white, then $S_{s_1}(\xi,\eta)$ is a constant which can be taken to be $S_{s_1}(0,0)$. This constant can be removed from the integrals of Equation (C-11); hence, the equation can be rewritten as

$$\frac{m_{s_4}^2}{\sigma_{s_4}^2} = \frac{\left(\iint_{-\infty}^{\infty} \left|H_1(\xi,\eta)\right|^2 d\xi \, d\eta \right)^2 \left(\iint_{-\infty}^{\infty} \left|H_2(\xi,\eta)\right|^2 d\xi \, d\eta \right)^2}{\iint_{-\infty}^{\infty} \left\{ \left|H_1(\xi,\eta)\right|^2 * \left|H_1(-\xi,-\eta)\right|^2 \right\} \left\{ \left|H_2(\xi,\eta) * H_2(-\xi,-\eta)\right|^2 \right\} d\xi \, d\eta} \quad . \tag{C-12}$$

If the spatial extent of $H_1(\xi,\eta)$ is large compared to the spatial extent of $H_2(\xi,\eta)$, i.e., a substantial amount of incoherent integration or smoothing is done, then $\left|H_1(\xi,\eta)\right|^2 * \left|H_1(-\xi,-\eta)\right|^2$ can be considered a constant in the integral in the denominator of Equation (C-12) and the constant can be taken outside the integral sign. Thus, if the peak value of

$$\left\{ \left|H_1\right|^2 * \left|\overline{H}_1\right|^2 \right\}_{max} = \iint_{-\infty}^{\infty} \left|H_1(\xi,\eta)\right|^4 d\xi \, d\eta$$

is used, the ratio can be rewritten as

$$\frac{m_{s_4}^2}{\sigma_{s_4}^2} = \frac{\left(\iint_{-\infty}^{\infty} |H_1(\xi,\eta)|^2 \, d\xi \, d\eta \right)^2}{\iint_{-\infty}^{\infty} |H_1(\xi,\eta)|^4 \, d\xi \, d\eta} \cdot \frac{\left(\iint_{-\infty}^{\infty} |H_2(\xi,\eta)|^2 \, d\xi \, d\eta \right)^2}{\iint_{-\infty}^{\infty} |H_2(\xi,\eta) * H_2(-\xi,-\eta)|^2 \, d\xi \, d\eta} \tag{C-13}$$

Equation (C-13) can be rewritten in another form using the following relation. Let

$$Q(\xi,\eta) = H_2(\xi,\eta) * H_2(-\xi,-\eta) \quad ,$$

then by Parseval's theorem,

$$\iint_{-\infty}^{\infty} |Q(\xi,\eta)|^2 \, d\xi \, d\eta = \iint_{-\infty}^{\infty} |q(x,y)|^2 \, dx \, dy \quad ,$$

where $q(x,y)$ is the inverse Fourier transform of $Q(\xi,\eta)$. Thus Equation (C-13) becomes

$$\frac{m_{s_4}^2}{\sigma_{s_4}^2} = \frac{\left(\iint_{-\infty}^{\infty} |H_1(\xi,\eta)|^2 \, d\xi \, d\eta \right)^2}{\iint_{-\infty}^{\infty} |H_1(\xi,\eta)|^4 \, d\xi \, d\eta} \cdot \frac{\left(\iint_{-\infty}^{\infty} |h_2(x,y)|^2 \, dx \, dy \right)^2}{\iint_{-\infty}^{\infty} |h_2(x,y)|^4 \, dx \, dy} \tag{C-14}$$

To calculate actual values of $m_{s_4}^2/\sigma_{s_4}^2$ the forms of the coherent and incoherent apertures must be specified. The case of interest here is one in which circular apertures are used for both the coherent and incoherent imaging. Thus, assume H_1 and H_2, the Fourier transform of h_1 and h_2 respectively are circular apertures of diameter d and d/α. Or

$$H_1(f_\rho, f_\theta) = \begin{cases} 1 & |f_\rho| \le d/2 \\ 0 & |f_\rho| < d/2 \end{cases} \tag{C-15}$$

and

$$H_2(f_\rho, f_\theta) = \begin{cases} 1 & |f_\rho| \leq \frac{d}{2\alpha} \\ 0 & |f_\rho| > \frac{d}{2\alpha} \end{cases} \qquad \text{(C-16)}$$

The Fourier transform of H_2 is given by

$$h_2(x,y) = \int_{-\infty}^{\infty}\int H_2(f_\rho, f_\theta) e^{j2\pi(f_x x + f_y y)} \, dx \, dy$$

or because H_2 is circularly symmetrical,

$$h_2(\rho) = 2\pi \int_0^{d/2\alpha} r \, J_0(2\pi r\rho) \, dr \quad .$$

Let $r' = 2\pi\rho r$, then when $r = d/2\alpha$, $r' = \pi\rho d/\alpha$, and

$$h_2(\rho) = 1/2\pi\rho^2 \int_0^{\pi d\rho/\alpha} r' \, J_0(r') \, dr'$$

and because

$$\gamma \, J_1(\gamma) = \int_0^{\gamma} \xi \, J_0(\xi) \, d\xi$$

$$h_2(\rho) = \frac{\pi d^2}{2\alpha^2} \frac{J_1(\pi d\rho/\alpha)}{\pi d\rho/\alpha} \qquad \text{(C-17)}$$

Substituting Equations (C-15) and (C-17) into Equation (C-14) yields

$$\frac{m_{s_4}^2}{\sigma_{s_4}^2} = \frac{\left(\int_0^{2\pi} \int_0^{d/2} f_\rho \, df_\rho \, df_\theta \right)^2}{\int_0^{2\pi} \int_0^{d/2} f_\rho \, df_\rho \, df_\theta} \cdot \frac{\left[\int_0^{2\pi} \int_0^{\infty} \left(\frac{\pi d^2}{2\alpha^2} \right)^2 \left(\frac{J_1(\pi d\rho/\alpha)}{\pi d\rho/\alpha} \right)^2 \rho \, d\rho \, d\theta \right]^2}{\int_0^{2\pi} \int_0^{\infty} \left(\frac{\pi d^2}{2\alpha^2} \right)^4 \left(\frac{J_1(\pi d\rho/\alpha)}{\pi d\rho/\alpha} \right)^4 \rho \, d\rho \, d\theta}$$

which simplified to

$$\frac{m_{s_4}^2}{\sigma_{s_4}^2} = \frac{\alpha^2}{2} \cdot \frac{\left[\int_0^{\infty} \left(\frac{J_1(r)}{r} \right)^2 r \, dr \right]}{\int_0^{\infty} \left(\frac{J_1(r)}{r} \right)^4 r \, dr} \quad . \tag{C-18}$$

The integral in the numerator can be evaluated directly as

$$\left(\int_0^{\infty} \left(\frac{J_1(r)}{r} \right)^2 r \, dr \right)^2 = \frac{1}{4} \quad .$$

The value of the integral in the denominator can be evaluated by noting that circ(r) and $J_1(2\pi\rho)/\rho$ are Fourier transform pairs, where circ(r) = 1 for $r \leq 1$ and is equal to 0 otherwise.* Thus,

$$\int_0^{\infty} \left(\frac{J_1(r)}{r} \right)^4 r \, dr = \int_0^{2} \left| \frac{\text{circ}(r) * \text{circ}(r)}{2\pi} \right|^2 r \, dr$$

Because [12]

$$\frac{\text{circ}(r) * \text{circ}(r)}{2\pi} = \frac{\cos^{-1}(\rho/2) - \rho/2 \sqrt{1 - (\rho/2)^2}}{\pi}$$

*The integral was evaluated by Robert Bayma in a private communication.

$$\int_0^{\infty} \left(\frac{J_1(r)}{r}\right)^4 r\, dr = \int_0^{2\pi} \left[\frac{\cos^{-1}(\rho/2) - (\rho/2)\sqrt{1 - (\rho/2)^2}}{\pi}\right] \rho\, d\rho \quad .$$

By substituting $\rho = 2 \cos \alpha$, the following is obtained:

$$\int_0^{\infty} \left(\frac{J_1(r)}{r}\right)^4 r\, dr = \int_0^{\pi} \left[\frac{\alpha - \sin \alpha}{2\pi}\right] \sin \alpha\, dx$$

$$= \frac{1}{8} - \frac{2}{3\pi^2} = 0.05745 \quad .$$

Using these results, it follows that

$$\frac{m_{s_4}^2}{\sigma_{s_4}^2} = 2.18\, \alpha^2 = 2.18\, \frac{A}{a} \qquad \text{(C-19)}$$

where A is the area of the coherent aperture and a is the area of the aperture used for the incoherent low-pass filtering. Finally, the following can be written:

$$\frac{m_{s_4}}{\sigma_{s_4}} = 1.48\, \frac{D}{d} \qquad \text{(C-20)}$$

where D is the diameter of the aperture used in the coherent imaging step while d is the diameter of the aperture used in the incoherent low-pass filtering process.

REFERENCES

1. Laser Speckle and Related Phenomena, edited by J. C. Dainty, New York: Springer Verlag, 1975.

2. Upatnieks, J. and Lewis, R. W. "Noise Suppression in Coherent Imaging," Appl. Opt., Volume 12, 1973, p. 2161.

3. George, N. and Jain, A., "Speckle Reduction Using Multiple Tones of Illumination," Appl. Opt., Volume 12, 1973, p. 1202.

4. Lewis, R. W., Redundancy in Coherent Imaging Systems, Ph.D. Thesis, University of Michigan, 1973.

5. Dainty, J. C., "Detection of Images Immersed in Speckle Noise," Opt. Acta., Volume 18, 1971, p. 327.

6. Young, M., Faulkner, B., and Cole, J., "Resolution in Optical Systems Using Coherent Illumination," J. Opt. Soc. Amer., Volume 60, 1970, p. 137.

7. Johnson, J., "Analysis of Image Forming Systems," Image Intensifier Symposium, Fort Belvoir, Virginia, October 6-7, 1958, AD-220160.

8. Rose, A., Vision, Human and Electronic, New York: Plenum Press, 1974, pp. 19 and 97.

9. George, N., Jain, A., and Melville, R. D. S. Jr., "Speckle, Diffusers, and Depolarization," Appl. Phys., Volume 6, 1975, p. 65.

10. George, N., "Speckle," Optic News, Volume 2, p. 14.

11. Reed, I. S., "On a Moment Theorem for Complex Gaussian Processes," IRE Transactions on Information Theory, Volume IT-8, April 1962, pp. 194-195.

12. Goodman, J. W., Introduction to Fourier Optics, New York: Mc Graw-Hill, 1968.

DISTRIBUTION

	No. of Copies
Commander Defense Documentation Center Attn: DDC-TCA Cameron Station Alexandria, Virginia 22314	2
Commander US Army Research Office Attn: Dr. R. Lontz P. O. Box 12211 Research Triangle Park North Carolina 22709	2
US Army Research and Standardization Group (Europe) Attn: DRXSN-E-RX, Dr. Alfred K. Nedoluha Box 65 FPO New York 09510	2
US Army Materiel Development and Readiness Command Attn: Dr. Gordon Bushy Dr. James Bender Dr. Edward Sedlak 5001 Eisenhower Avenue Alexandria, Virginia 22333	1 1 1
Headquarters Hq DA (DAMA-ARZ) Washington, DC 20310	2
Director of Defense Research and Engineering Attn: Mr. L. Weisberg Washington, DC 20301	2
Director Defense Advanced Research Projects Agency 1400 Wilson Boulevard Arlington, Virginia 22209	1
Commander US Army Aviation Systems Command 12th and Spruce Streets St. Louis, Missouri 63166	1
Director US Army Air Mobility Research and Development Laboratory Ames Research Center Moffett, California 94035	1
Commander US Army Electronics Command Attn: DRSEL-TL-I, Dr. Jacobs -CT, Dr. R. Buser Fort Monmouth, New Jersey 07703	1 1
Director US Army Night Vision Laboratory Attn: John Johnson Fort Belvoir, Virginia 22060	1
Director Atmospheric Sciences Laboratory US Army Electronics Command White Sands Missile Range, New Mexico 88002	1
Director US Army Ballistic Research Laboratories Attn: Ken Richer Aberdeen Proving Ground, Maryland 21005	1
Commander US Army Combined Arms Combat Development Activity Fort Leavenworth, Kansas 66027	1
Commander US Army Frankford Arsenal Philadelphia, Pennsylvania 19137	1
Commander US Army Picatinny Arsenal Dover, New Jersey 07801	1
Commander US Army Tank Automotive Development Command Attn: DRDTA-RWL Warren, Michigan 48090	1
Commander US Army Mobility Equipment Research and Development Command Fort Belvoir, Virginia 22060	1
Commander US Army Harry Diamond Laboratories Attn: Dr. Stan Kulpa 2800 Powder Mill Road Adelphi, Maryland 20783	1
Commander US Army Armament Command Rock Island, Illinois 61202	1
Commander US Army Foreign Science and Technology Center Federal Office Building 220 7th Street, NE Charlottesville, Virginia 22901	1
Commander US Army Training and Doctrine Command Fort Monroe, Virginia 23351	1
Director Ballistic Missile Defense Advanced Technology Center Attn: ATC-D -O -R -T P. O. Box 1500 Huntsville, Alabama 35807	1 1 1 1
Commander US Naval Air Systems Command Washington, DC 20360	1
Chief of Naval Research Department of the Navy Washington, DC 20360	1
Commander US Naval Air Development Center Attn: Radar Division Warminster, Pennsylvania 18974	1
Commander US Naval Electronics Laboratory Center San Diego, California 92152	1
Commander US Naval Surface Weapons Center Dahlgren, Virginia 22448	1

	No. of Copies
Commander US Naval Weapons Center Attn: Mr. Robert Moore China Lake, California 93555	1
Director Naval Research Laboratory Attn: Code 5300, Radar Division, Dr. Skolnik Code 5370, Radar Geophysics Branch Code 5460, Electromagnetic Prop Branch Washington, DC 20390	1 1 1
Commander Rome Air Development Center US Air Force Attn: R. McMillan, OCSA James Wasielewski, IRRC Griffiss Air Force Base, New York 13440	1 1
Commander US Air Force, AFOSR/NP Attn: LT COL Gordon Wepfer Bolling Air Force Base Washington, DC 20332	1
Commander US Air Force Avionics Laboratory Attn: Don Rees CPT James D. Pryce, AFAL/WE Dr. B. L. Sowers, AFAL/RWI Wright Patterson Air Force Base, Ohio 45433	1 1 1
Commander AFGL Hanscom Air Force Base, Maryland 01731	1
Commander AFATL/LMT Eglin Air Force Base, Florida 32544	1
Hughes Research Laboratory Attn: Mr. Smith Mr. John F. Henry Mr. J. M. Baird 3011 Malibu Canyon Road Malibu, California 90265	1 1 1
Environmental Research Institute of Michigan Radar and Optics Division Attn: Dr. A. Kozma Dr. C. C. Aleksoff P. O. Box 618 Ann Arbor, Michigan 41807	1 1
University of Alabama Physics Department Attn: Dr. J. G. Castle 4701 University Drive, NW Huntsville, Alabama 35807	1
Institute of Defense Analysis Science and Technology Division Attn: Dr. Vincent J. Corcoran 400 Army-Navy Drive Arlington, Virginia 22202	1
Director Calspan Corporation Attn: R. Kell P. O. Box 235 Buffalo, New York 14221	1
California Institute of Technology Attn: Dr. N. George 1201 E. California Boulevard Pasadena, California	1
Optical Science Consultants Attn: Dr. D. L. Fried P. O. Box 388 Yorba Linda, California 92686	1
The Aerospace Corporation Attn: Dr. D. T. Hodges, Jr. 2350 East El Segundo Boulevard Los Angeles, California 90009	1
Commander Center for Naval Analyses Attn: Document Control 1401 Wilson Boulevard Arlington, Virginia 22209	1
Hughes Aircraft Company Missile System Group Attn: Dr. J. A. Glassman Canoga Park, California 91304	1
Goodyear Aerospace Corporation Arizona Division Attn: Mr. Fred Wilcox Mr. P. W. Murray Litchfield Park, Arizona 85340	1 1
Honeywell, Incorporated Systems and Research Division Attn: Dr. Paul Kruse Minneapolis, Minnesota 55413	1
Raytheon Company Attn: A. V. Jelalian 528 Boston Post Road Sudbury, Massachusetts 01776	1
Georgia Institute of Technology Engineering Experiment Station Attn: James Gallaper 347 Ferst Drive Atlanta, Georgia 30332	1
The Rand Corporation Attn: Dr. S. J. Dudzinsky, Jr. 1700 Main Street Santa Monica, California 90406	1
DRSMI-FR, Mr. Strickland -LP, Mr. Voigt -R, Dr. McDaniel Dr. Kobler -RBH -RB -RC -RD -RE -RE, Mr. Pittman -RF -RG -RH -RK -RN -RR, Dr. Hallowes Mr. Shapiro Mrs. Davis -RRE -Y -RBD -RPR (Record Set) (Reference Copy)	1 1 1 1 2 1 1 1 1 1 1 1 1 1 1 1 1 1 300 1 3 1 1